Insect Systematics and Diversity, (2022) 6(1): 6; 1–23
https://doi.org/10.1093/isd/ixab031
Research

ENTOMOLOGICAL SOCIETY OF AMERICA
SHARING INSECT SCIENCE GLOBALLY

OXFORD

Molecular phylogenetics, phylogenomics, and phylogeography

UCE Phylogenomics of New World *Cryptopone* (Hymenoptera: Formicidae) Elucidates Genus Boundaries, Species Boundaries, and the Vicariant History of a Temperate–Tropical Disjunction

Michael G. Branstetter[1,3] and John T. Longino[2,3]

[1]U.S. Department of Agriculture, Agricultural Research Service, Pollinating Insects Research Unit, Utah State University, Logan, UT 84322, USA, [2]School of Biology, University of Utah, Salt Lake City, UT 84112, USA, and [3]Corresponding authors, e-mail: michael.branstetter@usda.gov; jacklongino@gmail.com

Subject Editor: Jeffrey Sosa-Calvo

Received 8 June, 2021; Editorial decision 8 November, 2021

Abstract

The genus *Cryptopone* Emery contains 25 species of litter and soil ants, 5 of which occur in the Americas. *Cryptopone gilva* (Roger) occurs in the southeastern United States and cloud forests of Mesoamerica, exhibiting an uncommon biogeographic disjunction observed most often in plants. We used phylogenomic data from ultraconserved elements (UCEs), as well as mitogenomes and legacy markers, to investigate phylogenetic relationships, species boundaries, and divergence dates among New World *Cryptopone*. Species delimitation was conducted using a standard approach and then tested using model-based molecular methods (SNAPP, BPP, SODA, and bPTP). We found that *Cryptopone* as currently constituted is polyphyletic, and that all the South American species belong to *Wadeura* Weber, a separate genus unrelated to *Cryptopone*. A single clade of true *Cryptopone* occurs in the Americas, restricted to North and Central America. This clade is composed of four species that originated ~4.2 million years ago. One species from the mountains of Guatemala is sister to the other three, favoring a vicariance hypothesis of diversification. The taxonomy of the New World *Cryptopone* and *Wadeura* is revised. Taxonomic changes are as follows: *Wadeura* Weber is **resurrected**, with **new combinations** *W. guianensis* Weber, *W. holmgreni* (Wheeler), and *W. pauli* (Fernandes & Delabie); *C. guatemalensis* (Forel) (**rev. stat.**) is raised to species and includes *C. obsoleta* (Menozzi) (**syn. nov.**). The following **new species** are described: *Cryptopone gilvagrande*, *C. gilvatumida*, and *Wadeura holmgrenita*. *Cryptopone hartwigi* Arnold is transferred to *Fisheropone* Schmidt and Shattuck (**n. comb.**). *Cryptopone mirabilis* (Mackay & Mackay 2010) is a junior synonym of *Centromyrmex brachycola* (Roger) (**syn. nov.**).

Keywords: ultraconserved elements, taxonomy, ants, divergence dating, Mesoamerica

The Nearctic and Neotropical regions maintain largely distinct biotas at their extremes; however, the montane forests of Mesoamerica represent a biogeographic transition zone connecting the southern temperate zone with the northern tropics (Halffter 1987). North-south trending mountains have functioned variously as dispersal corridors and refugia for cold-adapted species over millions of years, including during recent glacial cycles. One intriguing biogeographic pattern in this transition zone is the existence of flora and fauna that occur in the forests of both eastern North America and the cloud forests of Mexico and Central America, often with a gap in the middle of the range. This pattern has been documented in over 50 plant species (Graham 1999), including in sweetgum trees (Morris et al. 2008, Ruiz-Sanchez and Ornelas 2014), and in a few animal species (Carlton 1990, Arbogast 2007). The pattern generally applies to single species or small clades and recent climatic events like global cooling and Pleistocene glaciation have been identified as important drivers of current distribution and genetic patterns.

Various hypotheses have been proposed to explain the distribution of temperate species in Mesoamerican cloud forests (Graham 1999, Ruiz-Sanchez and Ornelas 2014). One model posits that a

Version of Record, first published online January 25, 2022 with fixed content and layout in compliance with Art. 8.1.3.2 ICZN

widespread temperate forest existed in North America and fragmented after the early or middle Eocene (Axelrod 1975) or during repeated glacial cycles in the Quaternary (Zhao et al. 2013). The second hypothesis proposes dispersal or range expansion into suitable habitat from the north as climate cooled, either during the Pleistocene (Deevey 1949, Morris et al. 2010), Neogene (Graham 1999), or late Paleogene/early Neogene (Braun 1950). Examination of pollen records in Mesoamerica and the southeastern United States supports a north-to-south pattern of dispersal with plants being absent from Mesoamerica prior to the mid-Miocene when temperatures dropped substantially (Graham 1999). It is also possible that a mix of these hypotheses is true, with temperate species expanding into Mesoamerica during the Miocene and then fragmenting more recently during Pleistocene glaciation events, and perhaps dispersing again during warmer periods.

Among ant species, there are a couple of lineages that show the same temperate–tropical distribution pattern between the southeastern United States and the mountains of Mesoamerica. The genus *Stenamma* Westwood is diverse in the Holarctic and the mountains of Mesoamerica, but this connection is older, as evidenced by there being a distinct "Middle American" clade of species (Branstetter 2012, 2013). More akin to the pattern found in plants are lineages within the genera *Ponera* Latreille and *Cryptopone*. Both are cryptic members of a rarely collected leaf-litter ant fauna and both have species that exhibit disjunct distributions between the southeastern United States and Mesoamerican cloud forest. The genus *Ponera* was recently studied using phylogenomic data and was shown to have dispersed twice into North America (Branstetter and Longino 2019), with one of the lineages, represented by the single species *P. exotica* Smith, occurring from the eastern United States to Nicaragua. It was proposed that the species most likely dispersed southward along a corridor of cloud forest over the last 3.1 million years. *Cryptopone gilva* (Roger) has a similar distribution pattern to *P. exotica* (Longino 2006, Mackay and Mackay 2010); however, the phylogeny and species-level taxonomy of the genus, particularly in the Americas, remains poorly understood.

The genus *Cryptopone*, as currently defined, is a cosmopolitan genus with 25 species and one subspecies (Schmidt and Shattuck 2014, Bolton 2021), only five of which occur in the Americas. The workers are small, nearly or completely eyeless, and are part of a "cryptic" fauna found in soil, leaf litter, and rotting wood. *Cryptopone gilva* has been known for over a century as a species in the deciduous forest of the southeastern United States (e.g., Wheeler & Gaige 1920, Creighton & Tulloch 1930). It is very similar to the European *C. ochracea* (Mayr) and the two are considered closely related (Emery 1911). The westernmost record of *C. gilva* in the United States appears to be Montgomery County in east Texas (Wheeler and Wheeler 1985). Forel (1899) described *C. ochracea* r. *guatemalensis* from Guatemala, based on specimens from Guatemala and Nicaragua. Recent work has synonymized *C. ochracea* r. *guatemalensis* with *C. gilva* (Mackay & Mackay 2010) and revealed that *C. gilva* occurs not only as a common species in the eastern United States, but also as a moderately abundant species in cloud forests from southern Mexico to Costa Rica (Longino 2006, Mackay and Mackay 2010). *Cryptopone guianensis* (Weber), *C. holmgreni* (Wheeler), *C. mirabilis* (Mackay & Mackay), and *C. pauli* Fernandes & Delabie are rare species with largely South American distributions, although *C. guianensis* occurs as far north as Mexico.

Here we examine the systematics of *Cryptopone* in the Americas, based on molecular data and morphology. To elucidate both lineage and species diversity of *Cryptopone* in the Americas, we use ultraconserved element (UCE) phylogenomics to infer relationships among the American species and a selection of Old World congeners. We also examine the phylogenetic structure among multiple populations of *C. gilva* across its range to investigate species boundaries and to elucidate the timing and mode of diversification in the clade. We specifically address if populations of *C. gilva* originated in the north and recently dispersed south (dispersal hypothesis), similar to *Ponera exotica* (Branstetter and Longino 2019), if the lineage was once widespread and later fragmented due to cooling temperatures and glaciation (vicariance hypothesis), or a combination of these. Our results show that 1) the genus is not monophyletic and needed to be redefined, 2) there are multiple cryptic species that are difficult to distinguish by morphology alone, and 3) a species in the Guatemalan highlands is sister to all other American species, suggesting vicariance rather than recent dispersal from north to south. We also show that molecular species delimitation methods consistently inflate species numbers beyond what is reasonable using an integrative approach. The results illustrate the power of UCE phylogenomics to reveal previously hidden patterns of speciation and biogeography.

Material and Methods

Morphological Examination and Taxonomy

This study was based on 402 separate species occurrence records. Almost all the specimens were from Winkler or Berlese samples of sifted leaf litter and rotten wood from wet forest habitats. Very few nest series are known. Most material was from large-scale biodiversity inventory projects in Central America and southern Mexico, spanning 25 years (Projects ALAS, LLAMA, and ADMAC). All locality, collection, and specimen data are available in Supp Table 1 (online only).

Observations were made at 63 × magnification with a Leica MZ12.5 dissecting microscope. Measurements were made with a dual-axis micrometer stage with output in increments of 0.001 mm. However, variation in specimen orientation, alignment of crosshairs with edges of structures, and interpretation of structure boundaries resulted in measurement accuracy to the nearest 0.01 mm. All measurements are presented in mm.

The only morphometric measurement used in this study is head width (HW), defined as the maximum width of the head in full face view, not including the eyes. Ant taxonomy typically includes a set of standard measurements (head length, scape length, etc.), but we did not see conspicuous differences in proportions among the different species, and we expected most of the measurements to be highly co-linear. We rely on sequence divergence for species delimitation and do not carry out a morphometric analysis here. The species clearly differ in mean HW, and we include it as an (albeit imperfect) identification aid.

All holotypes and paratypes associated with the new species described here have unique specimen-level identifiers ("specimen codes") affixed to each pin. Specimen codes should not be confused with collection codes, which are associated with particular collection events. When reported, collection codes follow the collector. Specimen collection data are derived from a specimen database and are not direct transcriptions of labels. Latitudes and longitudes, when present, are reported in decimal degrees, as a precise point (five decimal places) followed by an error term in meters. Images of holotypes, distribution maps, and all specimen data on which this paper is based are available on AntWeb (www.antweb.org).

Specimen repositories are referred to with the following acronyms:

BEBC	Brendon Boudinot, personal collection.
BMNH	The Natural History Museum, London, U.K.
CAS	California Academy of Sciences, San Francisco, CA, USA.
CPDC	Centro de Pesquisas do Cacau, Itabuna, Bahia, Brazil.
DEIC	Senckenberg Deutsches Entomologisches Institut [former Deutsches Entomologisches Institut], Müncheberg, Germany.
EAPZ	Escuela Agrícola Panamericana, Tegucigalpa, Honduras.
ECOSUR	Colección Entomológica de El Colegio de la Frontera Sur, Unidad San Cristóbal, Chiapas, Mexico.
IEXA	Colección Entomológica, Instituto de Ecología, A. C., Xalapa.
INBIO	Instituto Nacional de Biodiversidad, Costa Rica.
INPA	Instituto Nacional de Pesquisas da Amazônia, Manaus, AM, Brazil.
JTLC	John T. Longino, personal collection, University of Utah, Salt Lake City, UT, USA.
LACM	Los Angeles County Museum of Natural History, Los Angeles, CA, USA.
MCZC	Museum of Comparative Zoology, Cambridge, MA, USA.
MGBC	Michael Branstetter, personal collection, Logan, UT, USA.
MHNG	Muséum d'Histoire Naturelle, Geneva, Switzerland.
MUCR	Universidad de Costa Rica, San Pedro, Costa Rica.
MUSM	Universidad Nacional Mayor de San Marcos, Museo de Historia Natural, Lima, Peru.
MZSP	Museu de Zoologia da Universidade de São Paulo, São Paulo, Brazil.
NHMB	Naturhistorisches Museum, Basel, Switzerland.
PSWC	P. S. Ward, personal collection, University of California, Davis, CA, USA.
SAMC	South African Museum, Cape Town.
SSC	S. Salata, personal collection.
UCDC	University of California, Davis, CA, USA.
UNAM	Universidad Nacional Autónoma de México, Mexico D. F., Mexico.
USNM	National Museum of Natural History, Washington, DC, USA.
UVGC	Colección de Artrópodos, Universidad del Valle de Guatemala, Guatemala City, Guatemala.
WMC	William Mackay, personal collection.
ZMHB	Museum für Naturkunde der Humboldt-Universität, Berlin, Germany.

Integrative Species Delimitation Approach

Species were delimited using morphological, molecular, and biogeographic data. A final species delimitation was completed by identifying sets of specimens that 1) were morphologically similar, 2) formed monophyletic groups based on sequence data, and 3) showed evidence of being reproductively isolated in sympatry with other species, as demonstrated by morphological and/or molecular data. As discussed below, we also implemented molecular species delimitation methods based mainly upon the multispecies coalescent (MSC) model. These methods were performed to test species boundaries based on the listed criteria above and to examine the data for potential additional species. However, no additional species were delimited if they were not found in sympatry with another species and were not morphologically well differentiated.

Molecular Taxon Sampling

We selected 29 *Cryptopone* and 8 outgroup specimens for our molecular dataset (Table 1). Species of *Diacamma* Mayr, *Mayaponera* Schmidt & Shattuck, *Parvaponera* Schmidt & Shattuck, *Ponera*, *Pseudoponera* Emery, and *Simopelta* Mann were used as outgroups. *Cryptopone* specimens included one specimen of *C. butteli* Forel from Malaysia, one specimen of *C. ochracea* (Mayr) from Greece, one specimen of *C. guianensis* from Costa Rica, one specimen of the newly described *C. pauli* from Guyana, one specimen of a new *Cryptopone* species from South America (described here as *C. holmgrenita* **sp. nov.**), and 24 specimens of putative *C. gilva*. The *C. gilva* specimens were distributed from the southeastern United States to Costa Rica, in most cases single specimens from local populations. Data were newly generated for this study for 28 specimens and extracted from Branstetter et al. (2017) for 5 specimens, Branstetter and Longino (2019) for three specimens, and Longino and Branstetter (2020) for one specimen.

DNA Sequence Generation

We employed the UCE approach to phylogenomics (Faircloth et al. 2012, Faircloth et al. 2015, Branstetter et al. 2017), combining target enrichment of ultraconserved elements (UCEs) with multiplexed, next-generation sequencing. All UCE molecular work was performed following the UCE methodology described in Branstetter et al. (2017), which includes the following steps: DNA extraction, library preparation, UCE enrichment, sample pooling, and sequencing on an Illumina HiSeq 2500 (PE125 v4) at the University of Utah genomics core facility. For UCE enrichment we used an ant-customized bait set ("ant-specific hym-v2") targeting 2,524 UCE loci common across Hymenoptera (Branstetter et al. 2017). The utility of this bait set to resolve relationships, both deep and shallow, in ants has been demonstrated in several studies (Branstetter et al. 2017, Pierce et al. 2017, Ward and Branstetter 2017, Branstetter and Longino 2019).

UCE Matrix Assembly

After sequencing, the UCE data were demultiplexed by staff at the University of Utah bioinformatics core, and once received, the sequence data were cleaned, assembled, and aligned using the Phyluce package v1.6 (Faircloth 2016) according to the process outlined in Branstetter et al. (2017). Within the Phyluce environment, we used Illumiprocessor (Faircloth 2013) and Trimmomatic (Bolger et al. 2014) for quality trimming raw reads, Trinity v2013-02-25 (Grabherr et al. 2011) for *de novo* assembly of reads into contigs, and LASTZ v1.02 (Harris 2007) for identifying UCE contigs from all contigs. All optional Phyluce settings were left at default values for these steps. For the bait sequences file needed to identify UCE contigs, we used the ant-specific hym-v2 bait file. To calculate various assembly statics, including sequence coverage, we used scripts from the Phyluce package (*phyluce_assembly_get_trinity_coverage* and *phyluce_assembly_get_trinity_coverage_for_uce_loci*).

After extracting UCE contigs, we aligned each UCE locus using a stand-alone version of the program MAFFT v7.130b (Katoh and Standley 2013) and the L-INS-i algorithm. We then used a Phyluce script to trim flanking regions and poorly aligned internal regions using the program Gblocks (Talavera and Castresana 2007). The program was run with reduced stringency parameters (b1:0.5, b2:0.5, b3:12, b4:7). We then used another Phyluce script to filter the initial set of alignments so that each alignment was required to include data for 75% of taxa. This

Table 1. Voucher list of specimens used for DNA extraction and sequencing

Taxon	ExID	Country	Admin1	Latitude	Longitude	VoucherID
Cryptopone butteli[a]	EX1180	Malaysia	Sabah	4.74332	116.97303	CASENT0635385
C. gilva	EX1194	United States	Georgia	32.87234	−81.96362	CASENT0749266
C. gilva	EX1195	United States	South Carolina	33.28657	−81.69506	CASENT0749267
C. gilvagrande **sp. nov.**	EX1545	Guatemala	Baja Verapaz	15.21345	−90.21851	CASENT0614525
C. gilvagrande	EX1549	Honduras	Ocotepeque	14.45775	−89.06814	CASENT0617514
C. gilvatumida **sp. nov.**	EX1722	Mexico	Oaxaca	18.16842	−96.90289	CASENT0640768
C. gilvatumida	EX1723	Mexico	Veracruz	19.52307	−97.02789	CASENT0631951
C. gilvatumida	EX1725	Mexico	Puebla	19.91779	−97.60756	CASENT0641046
C. guatemalensis **stat. rev.**	EX1173	Mexico	Chiapas	15.72065	−92.94008	CASENT0609721
C. guatemalensis	EX1175	Honduras	Francisco Morazán	14.35444	−86.84444	CASENT0610825
C. guatemalensis	EX1176	Costa Rica	Puntarenas	10.30306	−84.81083	CASENT0618515
C. guatemalensis	EX1181	Honduras	Olancho	14.93368	−85.90361	CASENT0616283
C. guatemalensis	EX1189	Nicaragua	Nueva Segovia	13.97852	−86.18884	CASENT0633134
C. guatemalensis	EX1190	Nicaragua	Jinotega	13.76753	−85.02451	CASENT0628985
C. guatemalensis	EX1191	Nicaragua	Matagalpa	12.97426	−85.23400	CASENT0623898
C. guatemalensis	EX1546	Guatemala	Zacapa	14.94673	−89.27588	CASENT0633817
C. guatemalensis	EX1547	Guatemala	Suchitepéquez	14.54800	−91.19369	CASENT0612652
C. guatemalensis	EX1548	Honduras	Olancho	15.09490	−86.73987	CASENT0615521
C. guatemalensis	EX1550	Nicaragua	Jinotega	13.10976	−85.86765	CASENT0633877
C. guatemalensis	EX1551	Nicaragua	Jinotega	13.56922	−85.69738	CASENT0618536
C. guatemalensis	EX1556	Costa Rica	Heredia	10.23617	−84.11767	INB0003659343
C. guatemalensis	EX1561	Costa Rica	Heredia	10.26667	−84.08333	INB0003212306
C. guatemalensis	EX1724	Mexico	Veracruz	18.53338	−95.14960	CASENT0631779
C. guatemalensis	EX1728	Mexico	Veracruz	18.55908	−95.19550	CASENT0642925
C. guatemalensis	EX1726	Mexico	Puebla	19.91779	−97.60756	CASENT0641047
C. ochracea	EX1613	Greece	Crete	35.20198	24.39642	CASENT0637778
Diacamma rugosum[a]	EX1574	Malaysia	Sabah	4.74000	116.97500	CASENT0634818
Mayaponera arhuaca[c]	EX1435	Costa Rica	Heredia	10.42864	−84.01866	INBIOCRI001241794
Parvaponera darwinii[a]	EX1610	Malaysia	Sabah	4.96478	117.80465	CASENT0637361
Ponera exotica[b]	EX1632	United States	Georgia	30.86139	−84.06750	CASENT0637287
P. leae[b]	EX1558	Australia	Queensland	−16.92145	145.58543	JTLC000006828
P. sinensis nr.[b]	EX1625	China	Hong Kong	22.41595	114.12722	CASENT0761219
Pseudoponera stigma[a]	EX1576	Honduras	Gracias a Dios	15.70857	−84.86234	CASENT0613273
Simopelta andersoni[a]	EX1575	Costa Rica	Alajuela	10.30926	−84.72941	CASENT0635057
Wadeura guianensis	EX1562	Costa Rica	Heredia	10.30700	−84.05931	INB0003694616
W. holmgrenita **sp. nov.**	EX1627	Peru	Madre de Dios	−12.87530	−71.41095	CASENT0637779
W. pauli	EX1612	Guyana	Potaro-Siparuni	5.00851	−59.64133	CASENT0637806

Specimen data extracted from a) Branstetter et al. (2017), b) Branstetter and Longino (2019), and c) Longino and Branstetter (2020).

resulted in a final set of 2,232 alignments and 1,865,649 bp of sequence data for analysis. To calculate summary statistics for the final data matrix, we used a script from the Phyluce package (*phyluce_align_get_align_summary_data*).

UCE Phylogenomic Analysis

To partition the UCE data for phylogenetic analysis, we used the Sliding-Window Site Characteristics based on entropy approach (SWSC-EN) (Tagliacollo and Lanfear 2018), which uses a sliding window to partition UCE loci into right flank, core, and left flank regions. The theoretical underpinning of the approach comes from the observation that UCE core regions are conserved, while the flanking regions become increasingly more variable (Faircloth et al. 2012). After running SWSC-EN, the resulting data subsets were analyzed using PartitionFinder2 (Lanfear et al. 2012, Lanfear et al. 2017). For this analysis, we used the *rclusterf* algorithm, AICc model selection criterion, and the GTR+G model of sequence evolution. The resulting best-fit partitioning scheme included 1,460 data subsets and had a significantly better log likelihood than alternative partitioning schemes that we tested (SWSC-EN: −9,384,760.3; By Locus: −9,723,305.9; Unpartitioned: −9,869,901.6).

Using the SWSC-EN partitioning scheme, we inferred phylogenetic relationships of *Cryptopone* species with the maximum likelihood-based program IQ-Tree v1.6.8 (Nguyen et al. 2015). For the analysis we selected the "-spp" option for partitioning and the GTR+F+G4 model of sequence evolution. To assess branch support, we performed 1,000 replicates of the ultrafast bootstrap approximation (UFB) (Minh et al. 2013, Hoang et al. 2018) and 1,000 replicates of the branch-based, SH-like approximate likelihood ratio test (SH-aLRT) (Guindon et al. 2010). For these support measures, values ≥ 95% and ≥ 80%, respectively, signal that a clade is supported. The above analysis was repeated with the DNA matrix converted to RY-coding, which is a method that can reduce systematic bias due to base composition heterogeneity and saturation (Phillips and Penny 2003). For this analysis, we used the "-m MFP" option for model selection and the same SWSC-EN partitioning scheme.

To get an alternative assessment of relationships and branch supports, we conducted a coalescent-based species tree analysis on the dataset using the summary program ASTRAL-III v5.5.9 (Zhang et al. 2017). We first created a set of gene trees for the set of 2,232 UCE loci using IQ-Tree v1.6.8. These analyses were

performed in IQ-Tree using the ModelFinder (Kalyaanamoorthy et al. 2017) option "-m MFP," the AICc model selection criterion, and 1,000 UFB replicates. Once the gene trees were generated, we followed the recommendation of Zhang et al. (2017) and used Newick Utilities (Junier and Zdobnov 2010) to collapse branches with ≤ 50% bootstrap support. Using the modified gene trees, we performed a standard ASTRAL analysis, leaving all terminals as separate entities, and assessing support as local posterior probabilities.

Divergence Dating

We used BEAST2 v2.6.3 (Bouckaert et al. 2014) to estimate the timing of *Cryptopone* evolution in the New World. Due to computational constraints, we restricted our analysis to a subset of UCE loci and used a constraint tree. For the loci, we identified the 631 UCE loci that contained all samples (= 100% taxon occupancy) and then randomly selected 300 of these loci for analysis using a Phyluce script (*phyluce_align_randomly_sample_and_concatenate*). For the constraint tree, we used the best tree from the IQ-Tree analysis described above. Before importing the tree into BEAST2, we converted it to ultrametric by rooting the tree on *Mayaponera*+*Simopelta*, assigning the root node an age of 81.4 Ma, and performing a strict clock analysis using the *chronos* function in the R v3.4.4 (R Core Team 2019) package APE v5.4 (Paradis et al. 2004). The *chronos* function executes a fast penalized likelihood divergence dating method (Kim and Sanderson 2008, Paradis 2013).

To configure the BEAST2 analysis, we used the program BEAUti (included with BEAST2), and we applied two node-based calibration points. For the root node, we used a secondary calibration, extracting the age constraint from a comprehensive dating analysis of all ants (Economo et al. 2018), and we selected a normal distribution for the prior, assigning it a mean age of 81.4 Ma and a standard deviation of 6.07. For the other node calibration, we assigned two fossil species of *Ponera* from Baltic amber (Dlussky 2009) to the stem node of *Ponera*. For the prior, we selected a log normal distribution and assigned a Priabonian age to Baltic amber (see Perkovsky 2007; BEAST2 settings: offset = 33.9, mean = 3.16, stdev = 0.43). For the analysis, we used a GTR+G4 model of sequence evolution, an uncorrelated lognormal clock, and a birth-death tree prior. The birth-death tree prior was chosen because our dataset includes inter- and intraspecific sampling and a recent simulation study showed that, with this type of sampling, the birth-death model more accurately recovers ages (Ritchie et al. 2017). We set an exponential distribution for the *ucld mean* prior (mean = 1.0, initial value = 0.0025) and used default values for the remaining priors. For the *ucld stdev* prior we set the initial value to 0.5 based on information from preliminary runs. We performed seven independent runs, each for 200×10^6 generations, sampling every 5×10^3 generations. Run convergence was assessed using Tracer v1.7.1 (Rambaut et al. 2018) and runs were combined and summarized using LogCombiner and TreeAnnotator, respectively, with node heights calculated as mean heights. All runs converged, and with the burn-in set at 50%, all parameter values had effective sample sizes (ESSs) above 200. All BEAST2 runs were performed using the CIPRES Science Gateway (Miller et al. 2010).

Mitogenomic Analysis

We independently assessed *Cryptopone* phylogeny and species boundaries by assembling a separate mitochondrial DNA (mtDNA) dataset for analysis. This is possible because mtDNA and often entire mitogenomes can often be extracted from UCE data as bycatch (Ströher et al. 2017). We started by re-assembling the trimmed UCE sequences using the program SPAdes (Bankevich et al. 2012), which we have found to produce better results for this purpose. We then used the program MitoFinder (Allio et al. 2020) to locate, extract, and annotate all contigs containing mitochondrial sequence for all samples. As the reference for the MitoFinder analysis, we used a mitogenome of *Cryptopone sauteri* (Wheeler) (GenBank Accession# MK138572). To better extract the gene *cytochrome oxidase I* (COI) for all samples, we also used a Phyluce script (*phyluce_assembly_match_contigs_to_barcode*) to slice out sequence matching a reference, in this case we used a MitoFinder sequence from one our samples. The latter approach tends to work better at extracting individual genes but is not an efficient way to extract all mtDNA loci.

To expand our taxon sampling in this dataset, we downloaded COI barcode sequence data from the BOLD database (Ratnasingham and Hebert 2007), like the approach used in Longino and Branstetter (2020). We first searched BOLD for all samples matching the term "Cryptopone." We then searched in BOLD again using the BIN numbers resulting from the first search. This produced an initial set of 477 sequences. After performing a preliminary analysis, we filtered out many misidentified samples and selected a final set of 47 sequences of relevance to our study (Supp Table 3 [online only]). All of the retained sequenced were > 500 bp in length.

The BOLD COI sequences were combined with the MitoFinder sequences and all mtDNA loci were aligned individually using MAFFT. After alignment, the two ribosomal genes were trimmed using Gblocks and the protein coding genes were manually inspected and trimmed by eye. The loci were then concatenated and partitioned by gene and codon position. We analyzed the mtDNA dataset in IQ-Tree v2.1.2 using the "-m MFP+Merge" option for model selection and performed 1,000 UFB and SH-aLRT replicates for branch support. The final mtDNA supermatrix included 84 taxa and 12,861 bp of sequence data.

Legacy Marker Phylogenetic Analysis

Similar to the mtDNA analysis, we expanded the generic coverage of our dataset by extracting legacy exon markers from our UCE data and combined the results with published data available in GenBank. We extracted 14 legacy genes from a selection of 22 UCE samples using the approach described in Branstetter et al. (2017). We combined these sequences with data from 12 published studies (Ohnishi et al. 2003, Ward and Downie 2005, Brady et al. 2006, Moreau et al 2006, Oullette et al. 2006, Spagna et al. 2008, Schmidt 2013, Ward et al. 2015, Larabee et al. 2016, Ward and Fisher 2016, Matos-Maraví et al. 2018, Borowiec et al. 2019), including a comprehensive study of the subfamily Ponerinae by Schmidt (2013). After combining the data, each gene was aligned using MAFFT, trimmed using Gblocks, and visually inspected by eye using Mesquite. We then concatenated the data and analyzed the supermatrix in IQ-Tree v1.6.8 using a by-gene partitioning scheme, the GTR+F+G4 model of sequence evolution, and 1,000 UFB and SH-aLRT replicates for support. The final DNA supermatrix included 173 taxa and 11,361 bp of sequence data.

Phylogeny and Molecular Species Delimitation of the *C. gilva* Complex

As described in the Results section, we found that *C. gilva* has deep phylogenetic structure and likely constitutes multiple species. To further explore phylogenetic relationships and to test species boundaries within the *C. gilva* complex we created reduced datasets, in which we removed all samples except for specimens of *C. gilva* and the single outgroup *C. ochracea*. We then inferred phylogenies for

both UCE and mtDNA datasets and tested several different molecular species delimitation methods.

For phylogeny using the reduced UCE dataset, we repeated all matrix assembly steps described previously for UCE data and inferred a new SWSC-EN partitioned tree with IQ-Tree v1.6.8. We also generated a species tree by inferring gene trees and using ASTRAL, also as described previously. For the mtDNA dataset, we analyzed the full mitogenome dataset with reduced samples, but including the samples from BOLD, as described previously using IQ-Tree. We also created and analyzed a DNA barcode dataset, in which only 658 bp of the barcode region of *cytochrome oxidase I* (COI) was used for analysis. We partitioned the matrix by codon position and analyzed the data in IQ-Tree using GTR+G as the model of sequence evolution. The reduced UCE dataset, filtered to have 75% taxon completeness for each locus, included 2,199 UCE loci and 1,957,700 bp of sequence data. The reduced mitogenome dataset included 15 mtDNA loci and 12,765 bp of sequence data.

For molecular species delimitation in the *C. gilva* complex we tested multiple methods, including SNAPP (Bryant et al. 2012), BPP v4.0.4 (Yang 2015, Flouri et al 2018), SODA v1.0.1 (Rabiee and Mirarab 2021), and bPTP (Zhang et al. 2013). The program SNAPP is implemented in BEAST2 and is a full Bayesian program that estimates species trees from SNP data. It can also be used to delimit species by allowing all samples in a dataset to represent separate species. Interconnections among samples in the output trees, visualized using DensiTree, can indicate the boundary between species and population-level divergences. To identify and extract SNPS we phased the UCE data using the phasing pipeline implemented in Phyluce v1.6 (https://phyluce.readthedocs.io/en/latest/tutorials/tutorial-2.html) and described in Andermann et al. (2019). Phasing was performed by aligning the cleaned reads to all UCE contigs extracted from each sample. After phasing the data, we aligned the data matrix using MAFFT and the L-INS-i algorithm, we edge-trimmed the alignments using a Phyluce script (*get_trimmed_alignments_from_untrimmed*), and we filtered the alignments to have 75% taxon completeness. We then removed the outgroup *C. ochracea* from the alignments and used Phyluce to extract one random SNP per locus, allowing for missing data. We then converted the matrix to numerical "012" coding. This produced a matrix with 1,669 SNPs. The SNAPP analysis was set up and run using BEAUti and BEAST2 v2.5. We assigned each sample to its own species, left priors at default values and set the MCMC chain to run for $5x10^6$ generations, sampling every 100. After running the analysis, we examined the output logs in Tracer, combined tree files using a burnin of 10%, and examined the output using DensiTree, which is included with BEAST2.

Like SNAPP, the program BPP v4.0.4 is a Bayesian method that uses the multispecies coalescent (MSC) model to infer a species tree and delimit species (Yang 2015, Flouri et al 2018). However, instead of SNPs, the program takes full sequence alignments from multiple loci. For the analysis, we performed the A11 method which conducts a joint species tree estimation and species delimitation. We used 1,018 UCE loci for the analysis, which constitutes all loci with 100% taxon occupancy and at least 10 informative sites. Unlike the SNAPP analysis, we left in the single outgroup *C. ochracea* in the alignments. All samples were treated as potentially separate species and for the starting species tree we used the SWSC-EN partitioned tree output from IQ-Tree. We set burnin to 1×10^4 generations and collected $100x10^3$ samples, sampling every 2 generations. We performed two separate runs and examined the output for convergence. We then combined the run outputs and generated a final combined result.

Next, we used the program SODA v.1.0.1 (Rabiee and Mirarab 2021) to delimit species. This program is like ASTRAL and uses quartet frequencies from gene trees and the MSC model to infer species boundaries. Because it relies on already inferred gene trees to delimit species, it is much faster than BPP and other full Bayesian delimitation methods and has been found to be nearly as accurate. For this analysis we used the same set of 1,018 UCE loci used for BPP, with the clades receiving less than 50 UFB support collapsed into polytomies. We ran the program with a rooted guide tree based on the SWSC-EN partitioned analysis from IQ-Tree.

Lastly, we performed a set of species delimitation analyses using the Bayesian implementation of the PTP model (Zhang et al. 2013). This approach takes a rooted phylogenetic tree and models speciation in terms of number of substitutions. For the input trees, we tested the SWSC-EN partitioned UCE tree, the mitogenome tree, and the barcode-only tree, all inferred using IQ-Tree. For the analysis we used the bPTP server (https://species.h-its.org) and left input values at default. The outgroup was removed for each analysis.

Nomenclature

This paper and the nomenclatural act(s) it contains have been registered in Zoobank (www.zoobank.org), the official register of the International Commission on Zoological Nomenclature. The LSID (Life Science Identifier) number of the publication is urn:lsid:zoobank.org:pub:386C49F1-B004-41A5-BA32-F655E9A6FE28

Results

UCE Sequencing and Matrix Assembly

After sequencing, assembly, and the extraction of contigs representing UCE loci, we recovered an average per contig coverage of 41.6x (range: 9.1-63.3x) and a mean contig length of 889.5 bp (range: 651.9-1,045.1 bp). Following alignment, trimming, and filtering of the UCE contigs, our UCE matrix consisted of 2,232 loci and 1,865,649 bp of sequence data, of which 532,456 bp were informative. The mean alignment length post-trimming was 835.9 bp (range: 232-2,311 bp). The final UCE matrix included only 15.8% missing data (including gaps). For additional assembly stats, see Supp Table 2 (online only).

UCE Phylogenetics of Cryptopone Lineages

Cryptopone as currently constituted is polyphyletic. All results, but particularly the UCE trees, show that the three sequenced South American specimens are distantly related to the North American specimens (Fig. 1; Supp Fig. 1 [online only]). The South American specimens are more closely related to the Old World genus *Parvaponera* and the Neotropical genus *Pseudoponera*. This result was unequivocally supported across all UCE analyses, including the RY-coded analysis (Supp Fig. 2 [online only]) and the ASTRAL species tree analysis (Supp Fig. 3 [online only]). North American *Cryptopone* (the *C. gilva* complex in Fig. 1) form a clade sister to the European species *C. ochracea*, and together they form a clade sister to *C. butteli*, a species from the Old World tropics. For the South American clade of *Cryptopone*, the genus name *Wadeura* is available and there are morphological features that support its separation (see Taxonomy).

Legacy Phylogenetics of Ponerinae

We successfully extracted most legacy loci from the 22 UCE specimens included in this dataset and combined these data with those from published data in GenBank. The final matrix included 173 taxa and 11,361 bp of sequence data and the IQ-Tree analysis returned a reasonable phylogeny that provides new insights into

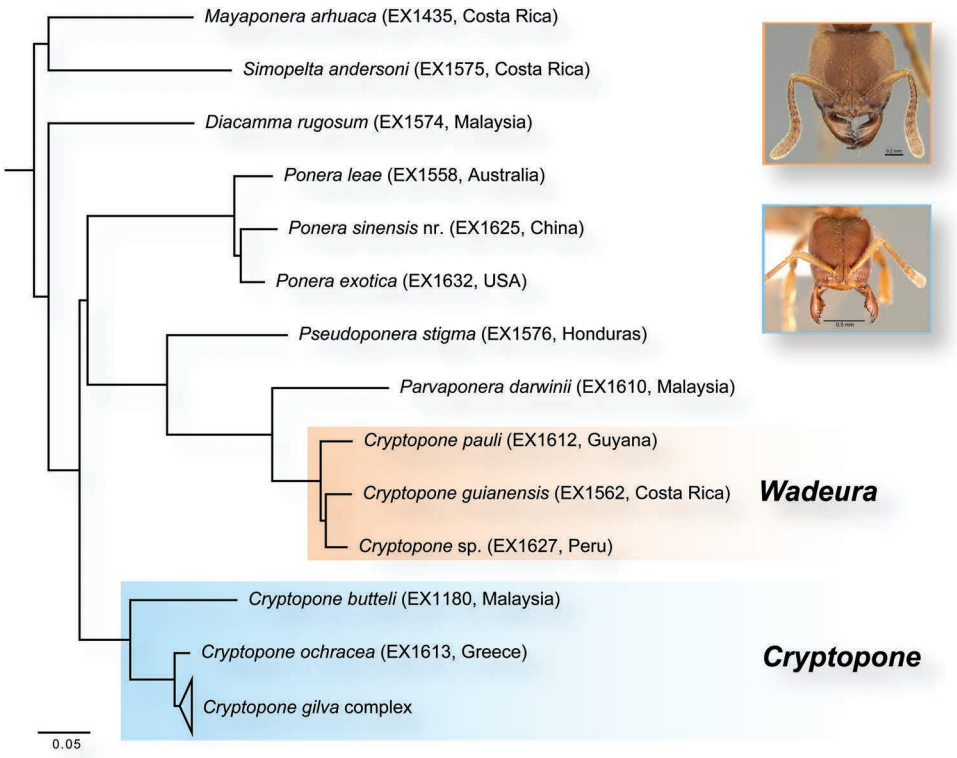

Fig. 1. Relationships among *Cryptopone* lineages based on analysis of 2,232 UCE loci and the SWSC-EN partitioning scheme. Among lineages, the South American clade is separate from the North/Central American clade of *Cryptopone* and they are not closely related. The constituent species of the South American clade are transferred to the resurrected genus *Wadeura*. All node support values are at maximum (UFB/SH-aLRT values of 100/100). The photo insets are of *Wadeura holmgreni* (CASENT0373370, Credit: Michelle Esposito) and *C. gilva* (CASENT0003325, Credit: April Nobile). The same tree with support values is available in Supp Fig. 1 (online only).

the systematics of Ponerinae. Focusing on *Cryptopone*, we find further support for *Cryptopone* polyphyly. The results largely mirror those of the UCE data except that, because of the expanded taxon set, the separation between South American and North American *Cryptopone* lineages is greater, with a larger diversity of ponerine genera in between (Fig. 2; Supp Fig. 7 [online only]). The analysis also revealed a third *Cryptopone* lineage, represented by *C. hartwigi* Arnold, as being sister to the genus *Fisheropone* Schmidt & Shattuck and more distantly related to the other *Cryptopone* lineages. Consequently, *Cryptopone* as currently defined, is polyphyletic, and composed of three distinct lineages. Within North American *Cryptopone*, the exon tree recovered the same result as the UCE data except that *C. ochracea* plus *C. sauteri*, a species from Taiwan, form a clade that is sister to the *C. gilva* complex.

UCE Phylogenetics of the *C. gilva* Complex

Relationships within the *C. gilva* complex were consistently resolved across both the full and reduced UCE datasets, with only minor incongruences across analyses (Fig. 3; Supp Figs. 1–5 [online only]). All analyses recovered four main clades, which we, taking into account morphology and distribution (i.e., sympatry), ultimately delimit as species (but see species delimitation results below). A new species from the Mesoamerican highlands, *C. gilvagrande*, is sister to a *C. gilva* clade that occurs from the southern United States to Costa Rica. The *C. gilva* clade comprises *C. gilva*, from the southern United States, and a *C. guatemalensis* clade that occurs from Mexico southward. The *C. guatemalensis* clade further divides into a widespread *C. guatemalensis* and, in the northern portion of the range, a sympatric new species, *C. gilvatumida*.

Within *C. guatemalensis* there is evidence of phylogeographic structure. Most analyses recovered a specimen (EX1726) from Mexico's Sierra Oriental as sister to the remaining specimens. The sister clade divides into northern and southern clades. The northern clade has two subclades, one joining Sierra de Los Tuxtlas in Veracruz, Mexico, with a specimen from southern Guatemala, and one with specimens from the Sierra de Chiapas and western Guatemala. The southern clade divides into one cluster of very closely related specimens from Honduras and northern Nicaragua, and a second cluster from Costa Rica. Across analyses, there was some topological instability within the Honduras/Nicaragua clade of specimens, but these relationships were shallow and did not receive maximum support (Fig. 3; Supp Figs. 1–5 [online only]).

mtDNA Phylogenetics of *Cryptopone*

We successfully recovered most mtDNA loci from all UCE samples, and we recovered the barcode region of COI for all samples. There was a total of 15 mtDNA loci included in analyses, and combined with the data from BOLD, the complete mitogenome matrix included 84 taxa and 12,861 bp of sequence data. The reduced mitogenome matrix included only 55 taxa and 12,765 bp of sequence data. The barcode only matrix included the same number of taxa, but only 658 bp of sequence data. Both the full and reduced mtDNA datasets recovered topologies consistent with the UCE results (Fig. 4; Supp Figs. 8–10 [online only]). Although relationships among distant outgroups varied, and were poorly supported, the mtDNA tree

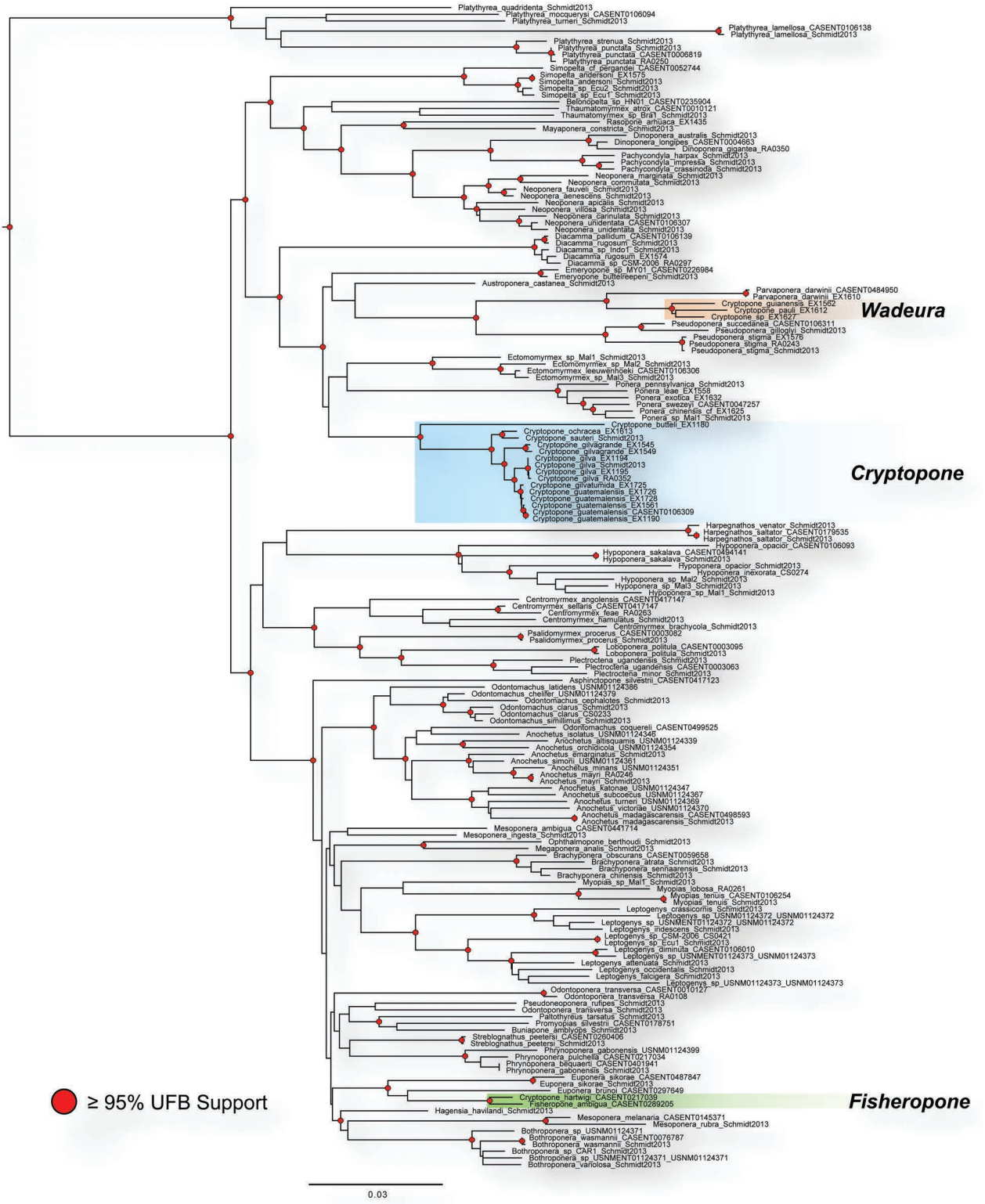

Fig. 2. Phylogeny of Ponerinae inferred with IQ-Tree using a dataset consisting of 14 legacy genes compiled from UCE sample data and published samples available in GenBank. The full matrix included 173 taxa and 11,361 bp of sequence data. *Cryptopone* separates into three lineages consisting of a South American clade (= *Wadeura*), a North/Central American clade (= *Cryptopone*), and the species *Cryptopone hartwigi* (= *Fisheropone;* see Taxonomy for more detail). Red circles on nodes indicate UFB support values ≥95%. Our support values are not shown but are available in Supplemental Material (Supp Fig. 7 [online only]). Codes at the end of taxon names correspond to either voucher specimen codes found in GenBank, extraction codes used in this study, or a particular study.

resolves *Cryptopone* into two clearly separated lineages (one being *Wadeura*), mirroring the UCE results (Supp Fig. 8 [online only]). Within the *C. gilva* complex, the reduced mitogenome tree resolved samples into four main clades, congruent with the UCE results and our final species delimitation (Fig. 4; Supp Fig. 9 [online only]). The full mitogenome tree (Supp Fig. 8 [online only]) and the barcode only

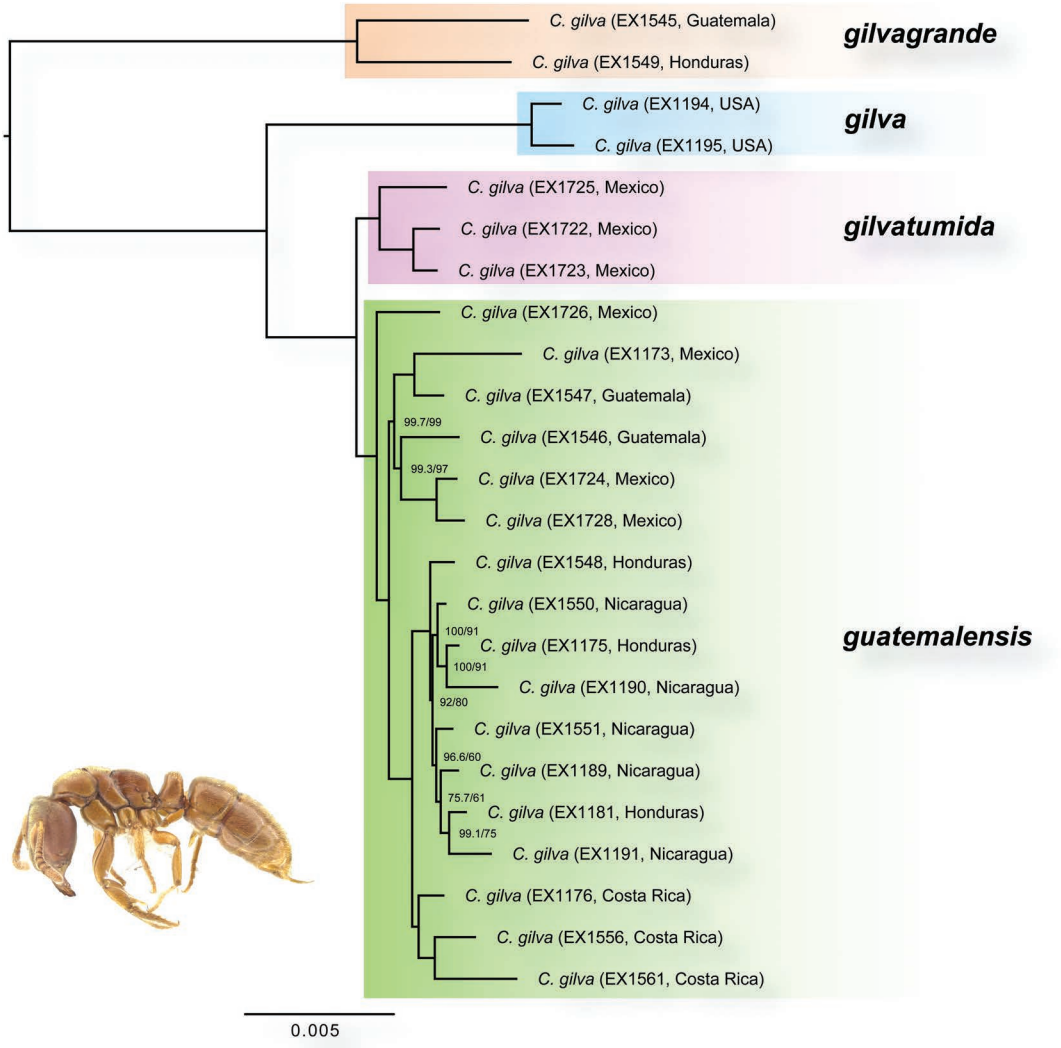

Fig. 3. Relationships among samples within the *C. gilva* complex based on analysis of 2,199 UCE loci and the SWSC-EN partitioning scheme. Four main clades were recovered and these were delimited as species using an integrative approach. Support values are UFB/SH-aLRT with maximum supports (100/100) not shown. The photo inset is of *C. guatemalensis* (CASENT0646802; Credit: John Longino). The same tree with support values is available in Supp Fig. 2 (online only).

tree (Supp Fig. 10 [online only]), however, had one incongruence. Two *C. guatemalensis* specimens from Los Tuxtlas, Mexico, were recovered as sister to a clade with the remaining *C. guatemalensis* and *C. gilvatumida*, rendering *guatemalensis* paraphyletic. This result received only low support, indicating phylogenetic uncertainty possibly due to low information content or saturation. There was additional incongruence among relationships within the *C. guatemalensis* clade, but most of these relationships were also poorly supported. By including the BOLD samples in phylogenetic analyses, we identified several additional specimens of *Wadeura* and *C. guatemalensis* from Guanacaste, Costa Rica. The *C. guatemalensis* samples from Guanacaste form a single genetically homogenous clade, separate from the other Costa Rican *C. guatemalensis* samples.

Molecular Species Delimitation of the *C. gilva* Complex

The species delimitation analyses estimated there to be between 4 and 17 species (Fig. 5). The SNAPP analysis recovered a species tree consistent with the UCE phylogenetic results, in that it recovered the four main clades in the *C. gilva* complex. Within the *C. guatemalensis* complex, the analysis resolved the Honduras/Nicaragua and Costa Rica clades, but it did not clearly resolve relationships among the other specimens. This result supports the existence of at least four species in the *C. gilva* complex. The BPP analysis inferred a delimitation of 13 species with highest posterior probability and the summary program SODA estimated 16 species. For the bPTP analyses, 4 species were inferred for the UCE phylogeny, 17 for the mitogenome phylogeny (only 13 species represented in the UCE tree), and 15 for the barcode only phylogeny (only 12 represented in the UCE tree). The four species inferred for the UCE phylogeny do not correspond to the same species that we ultimately delimited here. The analysis separated *C. gilvagrande* into one species, merged *C. guatemalensis* and *C. gilvatumida* into one species, and left *C. gilva* as one species. Across analyses, *C. gilvagrande* was consistently divided into two species, with *C. gilva* treated as a single species, *C. gilvatumida* separated into two species, and *C. guatemalensis* separated into multiple species. These results indicate that our final species delimitation of four species is a conservative estimate for the *C. gilva* complex.

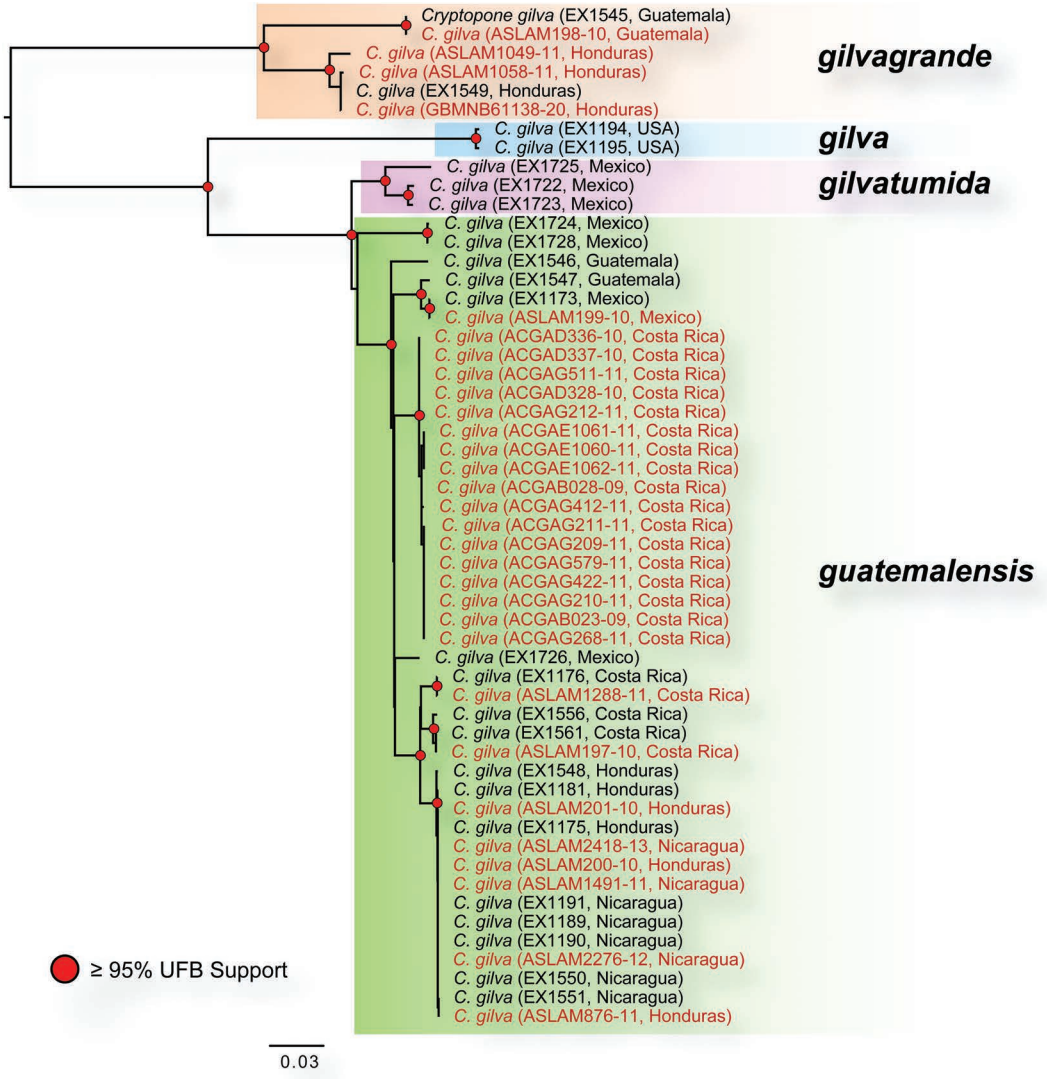

Fig. 4. Mitogenome phylogeny of the *C. gilva* complex inferred using 15 mtDNA loci and a merged partitioning scheme. Phylogeny includes mitogenomic data from UCE (black) samples and COI data only from BOLD (red) samples. Red circles on nodes indicate UFB support values of 95% or greater. The same tree with all support values is available in Supp Fig. 9 (online only).

Divergence Dating

The BEAST divergence dating analysis suggests that *Wadeura* has been separate from *Cryptopone* since the Paleocene, approximately 60.6 Ma (48.6–72.2 Ma 95% Highest Posterior Density [HPD]) (Supp Fig. 6 [online only]). The New World *Cryptopone* separated from the European *C. ochracea* much more recently in the late Miocene, 6.3 Ma (4.0–8.9 Ma 95% HPD) (Fig. 6). Within the *Cryptopone gilva* complex, *C. gilvagrande* separated from its sister clade 4.2 Ma (2.5–6.4 Ma 95% HPD) in the Pliocene; *C. gilva* separated from the *C. guatemalensis* clade 2.0 Ma (1.1–2.8 Ma 95% HPD) in the Pleistocene; and the *C. guatemalensis*/*C. gilvatumida* split was 1.0 Ma (0.6–1.3 Ma 95% HPD), also within the Pleistocene.

Discussion

Prior to our study, the genus *Cryptopone* was known as a set of 25 species, globally distributed, and all sharing a similar morphology. They were all small, somewhat generalized ponerines, living in leaf litter or soil, with eyes vestigial to absent, and with stout "traction setae" on the mid tibia. Using UCE phylogenomics, we have revealed that the genus as defined was polyphyletic, with the "*Cryptopone*" morphology being displayed by three disparate lineages. For the New World members of the genus, we have shown that true *Cryptopone* contains species in North and Central America, and these are most closely related to other Old World *Cryptopone*. The South American species are in a separate clade that is distantly related to true *Cryptopone*. On subsequent inspection we were able to find subtle morphological characters in the female castes that separated the two clades (see Taxonomy). Our methods and findings highlight the power of an iterative approach to taxonomy and systematics, in which morphology guides the initial hypotheses of taxa and the selection of specimens for sequencing, UCE phylogenomics provide a more ample dataset that either reinforces or modifies the hypotheses, which then guide a new search for morphological correlates of taxa and a deeper understanding of morphological and phylogenetic diversity. We not only exposed polyphyly, resulting in a resolution of generic boundaries, we also revealed details of species-level diversification across the North American landscape.

A little over 6 Ma, during the late Miocene, a *Cryptopone* species occurred that was the common ancestor of *C. ochracea* and its

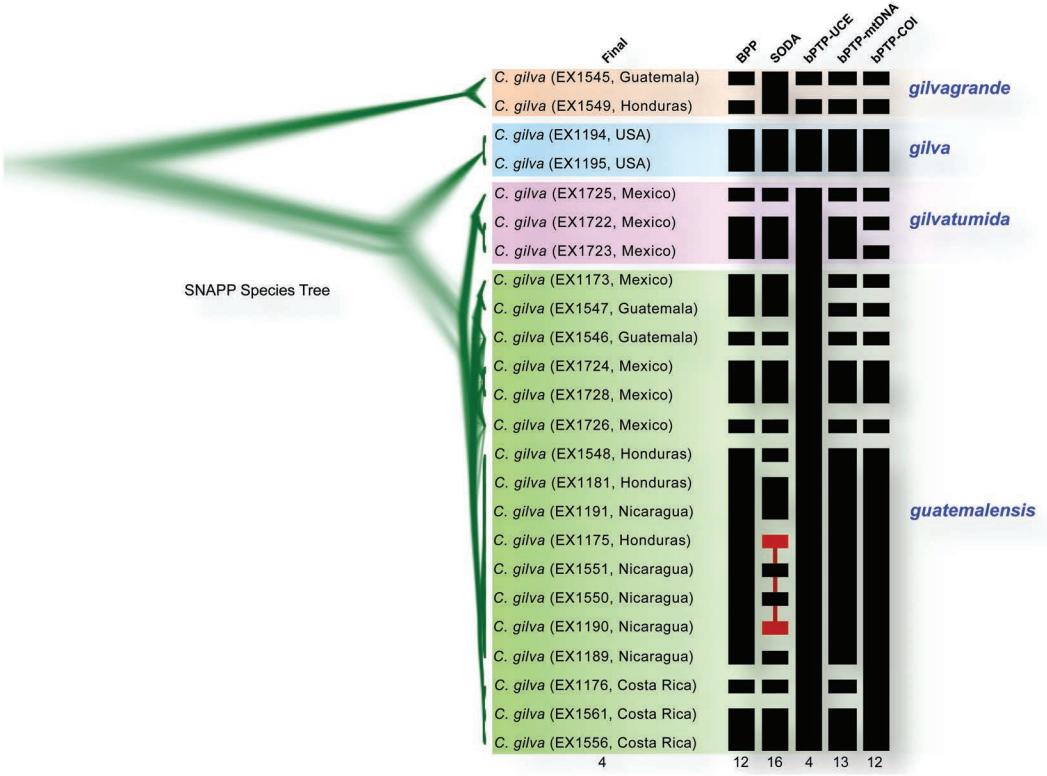

Fig. 5. Species tree and species delimitation in the *Cryptopone gilva* complex. The species tree was inferred using SNP data and the Bayesian program SNAPP, with the resulting tree set displayed using DensiTree. The SNAPP densitree shows at least four clearly differentiated species-level lineages. Species delimitation using the programs BPP, SODA, and bPTP, recovered between 4 and 17 species. The results for the UCE samples only are mapped onto the SNAPP densitree result. The connected red bars represent single species that were not monophyletic in the SNAPP phylogeny. The colored boxes and blue species names represent the final species delimitation and taxonomy.

sister taxon, the *C. gilva* complex. We do not know what the geographic range of that ancestral species might have been, particularly since we did not infer its distribution due to the small number of outgroup samples included here. However, we do know that the current distribution of *C. ochracea* is Europe, and the *C. gilva* complex is a New World radiation that occurs from the southeastern United States south to Costa Rica. Most of the species' diversity occurs in the Old World and the *C. gilva* complex is nested within them, suggesting that the ancestral home of the genus is presumably there. It is also reasonable to suggest that the origin of the *C. gilva* + *C. ochracea* clade is Holarctic, although this hypothesis needs to be confirmed with better outgroup sampling. Taking into consideration the various hypotheses presented in the introduction, we contrast dispersal and vicariance scenarios that could generate the current distribution and phylogeny of New World *Cryptopone* and suggest that vicariance of a once more widespread species, followed by some recent dispersal, is the most likely scenario for this group.

Dispersal with dispersal-associated speciation should produce a pectinate phylogeny. A dispersal front generates allopatric populations at the leading edge, resulting in reproductive isolation. Subsequent speciation occurs at the leading edge, leaving in its wake a series of individual species that do not continue to speciate. Thus each bifurcation in the phylogeny has one species to the North and a multi-species clade to the South. In this scenario, a *C. ochracea*-like ancestor disperses from Europe to eastern North America 6 Ma. The lineage spreads southward, differentiating and forming new species as it travels. In this case, *C. gilva* should be sister to the rest of the clade to the South, followed by *C. gilvatumida*, followed by *C. guatemalensis* and *C. gilvagrande* as the most recent speciation. This was what we expected, paralleling results for the litter ant *Ponera exotica* (Branstetter and Longino 2019). This scenario is not what we found in *Cryptopone*. Instead, we found a more complex pattern in which a species on mountaintops in Guatemala and Honduras was sister the rest of the *C. gilva* complex.

An alternative to the dispersal-speciation scenario, and one consonant with our phylogeny, is range expansion without speciation, followed by vicariance. In this scenario, a *C. ochracea* clade was Holarctic, extending across Eurasia and much of North America. Around 6 Ma, climate and sea-level change reduces the range and creates allopatric populations in Europe and North America. The North American population is widespread, extending south into Central America. Around 4 Ma, as global climate cooled and North Hemisphere ice sheets formed (Zachos et al. 2001), speciation occurs across elevational gradients in Central America, generating a large highland species (*C. gilvagrande*) and a widespread, smaller, middle-elevation species. About 2 Ma the latter subsequently divides into the northern *C. gilva* and a southern species, a result of Pleistocene cooling and consequent fragmentation of suitable mesic habitat. Finally, within the last one million years, the southern species further divides, generating a more cold-adapted *C. gilvatumida* in southern Mexico and a more tropical *C. guatemalensis* from southern Mexico to Costa Rica. This scenario is concordant with evidence that cloud forest habitat has oscillated up and down mountains during the Pleistocene, opening and closing dispersal pathways (Bush and Hooghiemstra 2005). Although fragmentation and vicariance explains the deeper biogeographic structure, there is still some evidence of a general north-to-south pattern of relationships within the species *C. guatemalensis* (Fig. 6). The southernmost populations

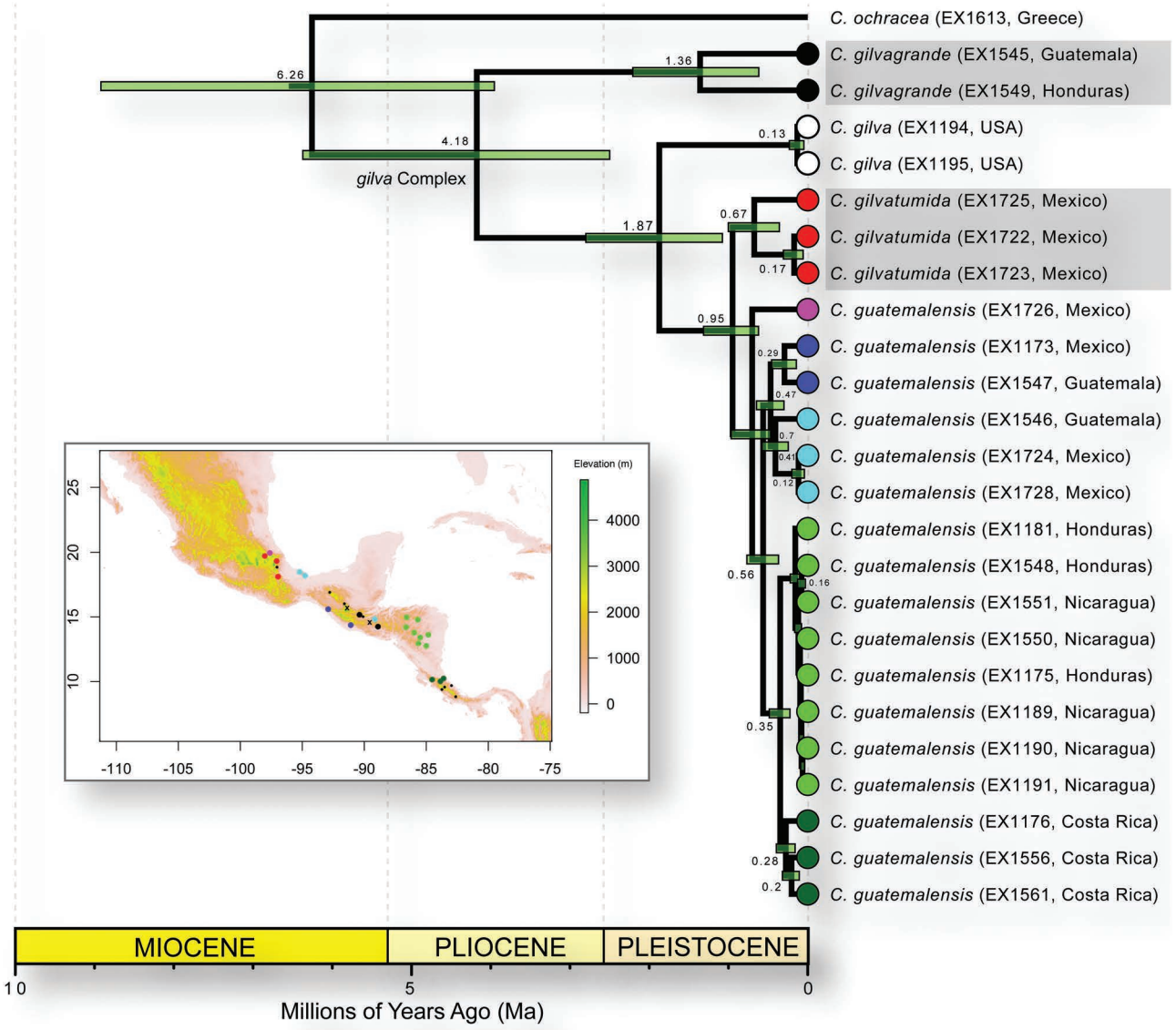

Fig. 6. Biogeography of the *Cryptopone gilva* complex within Central America. Chronogram inferred using BEAST2, 300 UCE loci, and a fixed topology (all UCE samples and SWSC-EN partitioning). Only results for the *C. gilva* complex are shown (see Supp Fig. 6 [online only] for the full results). Numbers on nodes are mean ages in millions of years ago and node bars are 95% Highest Posterior Densities (HPD). The map inset shows the distribution of *C. gilva*-clade samples within Central America. Colored dots match tip labels of the chronogram. Sites where specimens were identified by morphology alone (no sequencing) are shown as **x** for *C. gilvagrande* and a small black dot for *C. guatemalensis*. Samples of true *C. gilva* from the United States are not shown in the map.

of the *C. gilva* complex, which occur in Costa Rica, are nested within the complex and sister to a group of populations from nuclear Mesoamerica, in Honduras and Nicaragua. This group in turn is sister to a clade of species from Mexico and Guatemala.

Plant distributions and histories have been more thoroughly investigated, with examples of both dispersal and vicariance generating patterns of clade disjunctions between southeastern North America and the mountains of southern Mexico and Guatemala. Axelrod (1975) was an early proponent of vicariance, arguing that temperate elements in the Mexican highlands were the result of a once widespread temperate rainforest that had fragmented, and not the result of recent north to south migration. Ruis-Sanchez and Ornelas (2014) show for *Liquidambar styraciflua* that the greatest genetic diversity is in Mesoamerica, ruling out a recent dispersal to Mesoamerica from the north. They propose an older late Miocene arrival of temperate elements, consistent with conclusions of Braun (1950) and Graham (1999), who provide evidence that temperate elements were rare in Mesoamerica prior to this time based on the palynological record. *Cryptopone* may have been part of that temperate element. Separation of southeastern United States and Mesoamerican populations of *L. styraciflua* occurred later, in the Pleistocene, during periods of cooling and drying. The separation of southeastern *C. gilva* from the *C. guatemalensis* clade may have been coeval.

For species delimitation within the *C. gilva* complex, we used an integrative approach in which we considered data from morphology, distribution, and genetics to ultimately circumscribe four species, three of which are described as new to science. Without the molecular data it would have been nearly impossible to confidently resolve species boundaries in the *C. gilva* complex due to overlapping morphological variation among populations. To test our integrative delimitations, we explored the use of several molecular delimitation methods (SNAPP, BPP, SODA, bPTP) that ideally could resolve species boundaries using molecular data alone. Unfortunately, we found these approaches to be inconsistent and inflationary. The number of

delimited species ranged from 4 (bPTP-UCE) to 16 (SODA), with most methods, including the full Bayesian approach BPP, delimiting ≥ 12 species. These results could indicate the existence of more cryptic species, but it is also likely that at least some of these approaches are delimiting population structure rather than species boundaries, a noted problem for methods based on the multispecies coalescent model (Jackson et al. 2017, Sukumaran and Knowles 2017). Future work might benefit by including more samples (new localities and population samples) or by testing models like iBPP (Solís-Lemus et al. 2015) which combines morphometric and genetic data to delimit species. This approach was used in a recent study of *Temnothorax* ants and produced a more reasonable delimitation than the molecular data alone (Prebus 2021).

Taxonomy

Cryptopone Emery 1893

Type species: *Cryptopone testacea* Emery, 1893: cclxxv; by monotypy.

The phylogenetic results necessitate the revalidation of the genus *Wadeura* and consequent removal of the species *W. guianensis* **revived combination**, *W. holmgreni* **new combination**, and *W. pauli* **new combination** from *Cryptopone*. The shared characters of *Cryptopone* and *Wadeura* workers, as outlined by Schmidt and Shattuck 2014, are "frontal lobes small and closely approximated, scapes flattened, eyes vestigial to absent, propodeum with a distinct dorsal face which widens posteriorly, metabasitarsus with simple setae but lacking spiniform or peg-like traction setae, and mesotibiae with stout traction setae (sometimes small and reduced to a few, but always present)." Schmidt and Shattuck observed that most *Cryptopone* have a fovea or pit at the base of the mandible, with the exception of the *Wadeura*-like species. With the separation of *Wadeura*, the presence of a mandibular pit is apparently now universal in *Cryptopone*.

In *Cryptopone gilva* and relatives, the anterior face of abdominal sternite III has a pair of gibbosities ventral to the helcium, so that the helcium is "high" on the segment (Fig. 7A and B). These gibbosities are present on *C. ochracea* and *C. butteli*, species that we have been able to examine directly. Other *Cryptopone* species with images on AntWeb, including the type species *C. testacea*, show similar structure when the anterior face of abdominal sternite III is visible. This character may now be universal in *Cryptopone*. In *Wadeura*, there are no gibbosities and abdominal sternite III shallowly curves to the ventral rim of the helcium, so that the helcium is "low" on the abdominal segment (Fig. 7C and D). Although males are not treated here, there are substantial differences between the males of *Cryptopone* and *Wadeura* (B. Boudinot, pers. com.).

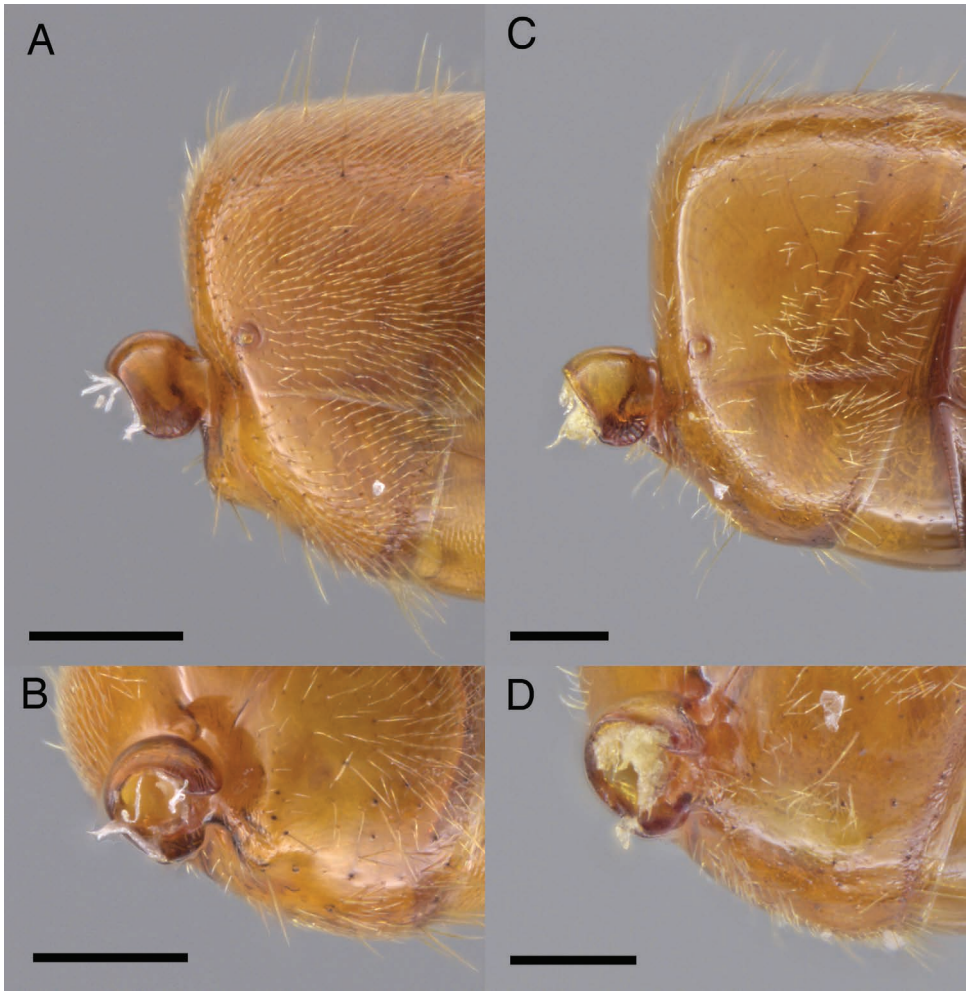

Fig. 7. Shape of third abdominal sternite, *Cryptopone* vs. *Wadeura*. *Cryptopone gilvagrande* (CASENT064143), lateral view (A), oblique ventral view (B). *Wadeura guianensis* (CASENT0640149), lateral view (C), oblique ventral view (D). Scale bars are 0.2 mm.

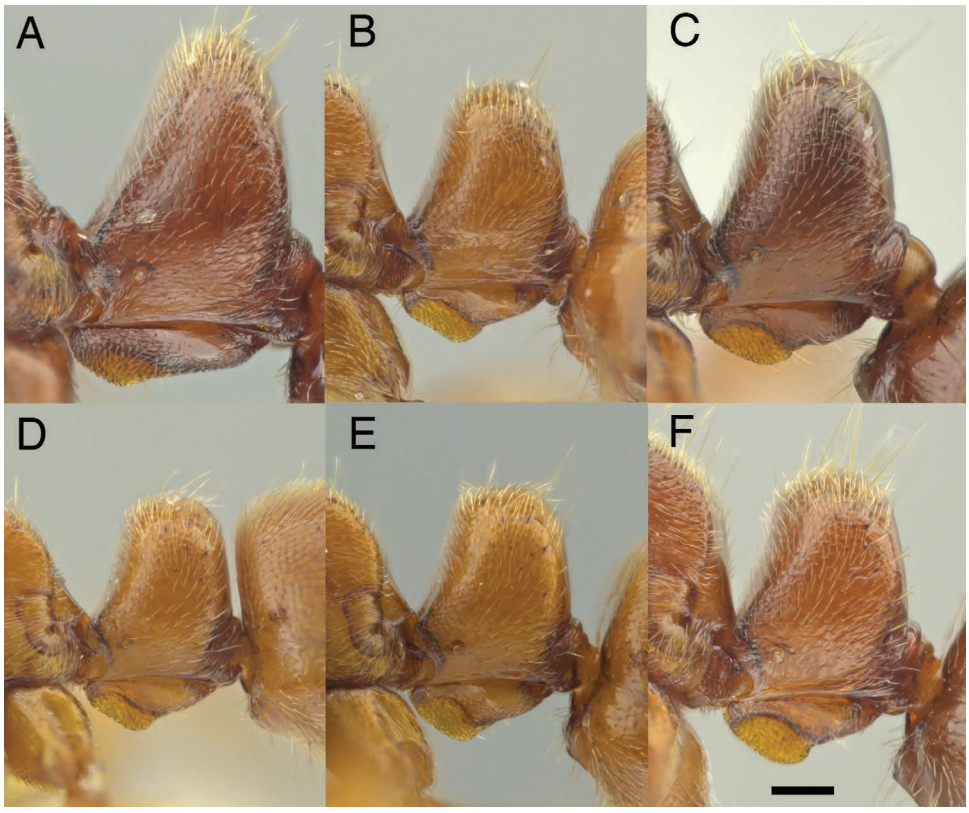

Fig. 8. Petiolar nodes of workers in the Mesoamerican members of the *C. gilva* complex. All images are to same scale (scale bar = 0.1 mm). (A) *C. gilvagrande* (CASENT0614525), Guatemala. (B) *C. gilvatumida* (CASENT0641046), Puebla, 1400 m. (C) *C. gilvatumida* (CASENT0631951), Xalapa, Mexico, 1940 m. (D) *C. guatemalensis* (CASENT0641031), Puebla, 1400 m. E. *C. guatemalensis* (CASENT0640429), Sierra de Los Tuxtlas, 1130 m. F. *C. guatemalensis* (CASENT0642925), Sierra de Los Tuxtlas, 1580 m. (B) and (D) occurred together in the same Winkler sample, and sequencing placed them in different clades.

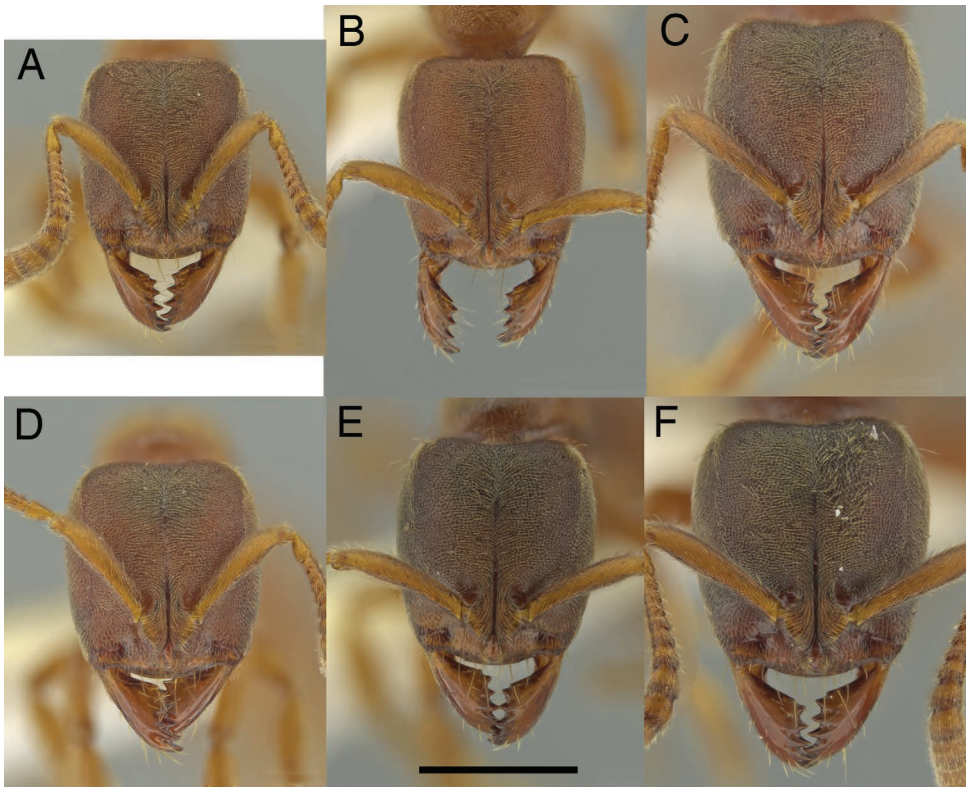

Fig. 9. Face views of workers in the *C. guatemalensis + C. gilvatumida* clade. All images are to same scale (scale bar = 0.5 mm). (A) *C. guatemalensis* (CASENT0641031), Puebla, 1400 m. (B) *C. guatemalensis* (CASENT0640429), Sierra de Los Tuxtlas, 1130 m. (C) *C. guatemalensis* (CASENT0642925), Sierra de Los Tuxtlas, 1580 m. (D) *C. gilvatumida* (CASENT0641046), Puebla, 1400 m. (E) *C. gilvatumida* (CASENT0641053), Puebla, 1790 m. F. *C. gilvatumida* (CASENT0631951), Xalapa, Mexico, 1940 m. (A) and (D) occurred together in the same Winkler sample, and sequencing placed them in different clades.

There is a single subsaharan species, *C. hartwigi* Arnold from South Africa. Although it has *Cryptopone* characters and habitus, Borowiec et al. (2019) and our phylogenetic results show it is in a clade of African ants separate from the rest of the genus. Our results show that it is sister to the African genus *Fisheropone*, to which we transfer it, as *F. hartwigi* **new combination**. Finally, *Cryptopone mirabilis* (Mackay & Mackay 2010) is shown to be a **junior synonym** of *Centromyrmex brachycola*.

With the removal of *Wadeura*, *F. hartwigi*, and the misplaced *C. mirabilis*, the genus *Cryptopone* is a more morphologically uniform set of species. This revised concept of *Cryptopone* has highest diversity in Asian and Indo-Malayan regions, with a few species extending into Palearctic and Nearctic regions. The Nearctic clade extends as far south as Costa Rica. *Cryptopone* is not present in South America.

We recognize four species of true *Cryptopone* in the Americas: *C. gilva*, *C. gilvagrande* **sp. nov.**, *C. gilvatumida* **sp. nov.**, and *C. guatemalensis* **rev. stat.**

Identification

Genetic diversification and divergence has occurred more rapidly than morphological divergence, and the four species recognized here are very uniform and not always differentiable based on morphology. The combination of sequence data and zones of sympatry support the recognition of multiple species. Multiple species within communities are often detectable because intrapopulational variation is low and individuals fall into discrete morphological clusters. Sequencing may then reveal that these local species are members of distinct clades, with the separate clades broadly distributed. However, geographic variation in both clades may blur morphological distinctions and prevent global diagnosis.

Key to Workers of American *Cryptopone*

1 HW > 0.8–0.96; petiolar node in side view relatively more tapering dorsally, ventral margin of petiole and anteroventral petiolar process relatively shallower (Fig. 8A); cloud forests of Guatemala and Honduras ..... *gilvagrande*

\- HW < 0.82; petiolar node less tapering, ventral margin of petiole and anteroventral petiolar process relatively more convex (Fig. 9B–F); USA to Costa Rica 2

2 (1) HW 0.74–0.80; southeastern USA ..... *gilva*

\- HW 0.57–0.82; Mexico to Costa Rica 3

3 (2) Petiolar node in side view slightly more tapering and rounded dorsally (Fig. 8B and C); HW 0.60–0.82; Puebla to Oaxaca, Mexico ..... *gilvatumida*

\- Petiolar node in side view slightly less tapering and more truncate dorsally (Fig. 8D–F); HW 0.57-0.73; Puebla, Mexico, south to Costa Rica ..... *guatemalensis*

Cryptopone gilva (Roger)

Ponera gilva Roger 1863:170. Syntype worker: U.S.A. [ZMHB, AntWeb image examined].
Pachycondyla (*Pseudoponera*) *gilva*: Emery 1901:46. *Euponera* (*Trachymesopus*) *gilva*: Emery 1911:86; Wheeler & Gaige 1920:70 (redescription of worker); Creighton & Tulloch 1930:74 (description of queen, male); Wheeler, G.C. & Wheeler, *Cryptopone gilva*: Brown 1963:3.
Pachycondyla gilva (part): Mackay & Mackay, 2010:352.
Euponera (*Trachymesopus*) *gilva* subsp. *harnedi* M. R. Smith 1929:543. Syntype worker: U.S.A., Mississippi, Columbus [USNM] (not examined). Synonymy by Creighton & Tulloch 1930:74.

Geographic range. Southeastern United States, from Tennessee and North Carolina south to Florida, west to Arkansas, Texas.

Measurements. *Worker* HW 0.75-0.80 (n=6).

Biology. This species occurs in a variety of mesic habitats in the southeastern United States. It nests in or under loose bark of rotten wood (Creighton and Tullock 1930). Colonies contain a few dozen to several hundred individuals and can be polygynous (Creighton and Tullock 1930; Haskins 1931; Smith 1934, 1944). Haskins (1931) provided an account of the behavior of a captive colony, with details of brood development and worker behavior.

Comments. Based on current distribution records, there is a significant distribution gap between *C. gilva* and the other American species of the *C. gilva* clade, but more information is needed on specimens from northern Mexico. The populations in the southeastern United States extend westward to Montgomery County in east Texas (Wheeler and Wheeler, 1985). There are no records further south in Texas. There is a record of a single specimen of *C. gilva* from Nuevo León, Mexico (Alatorre-Bracamontes and Vasquez-Bolaños 2010) and there are records of specimens from Jalisco (Vasquez-Bolaños 2011). We have not examined these specimens and do not know the

Fig. 10. Holotype of *Cryptopone gilvagrande* (unique specimen identifier CASENT0614525).

relationship of these to the *gilva*-clade species presented here. Our knowledge begins with our specimens from Puebla southwards.

Cryptopone gilva overlaps in size with *C. gilvatumida* and *C. guatemalensis*, and currently cannot be separated by morphology alone, but allopatry allows identification of *C. gilva* based on geography.

The distance between the two COI barcodes for this species was < 1%, and the smallest interspecific distance was 11%.

Cryptopone gilvagrande, New Species

(Figs. 6[map],8,9,10)

(Zoobank LSID: urn:lsid:zoobank.org:act:CD67CA6D-8BF0-470E-854C-EF12E2AC314B)

Type material. *Holotype worker*: Guatemala, Baja Verapaz, Biotopo Quetzal, 15.21345, –90.21851 ± 50 m, 1725 m, 7 May 2009, cloud forest, ex sifted leaf litter (LLAMA Wa-B-02-2-05) [USNM, unique specimen identifier CASENT0614525]. *Paratypes*: same data as holotype [1 worker, UVGC, CASENT0614526; 1 worker, CAS, CASENT0640156; 1 worker, MCZC, CASENT0640157; 1 worker, UNAM, CASENT0640158; 1 worker, UCDC, CASENT0640159].

Geographic range. Guatemala, Honduras.

Diagnosis. Worker HW > 0.79; petiolar node in side view tapering dorsally (Fig. 8A); ventral margin of petiole and anteroventral petiolar process shallow (Fig. 9A).

Measurements. *Worker* HW 0.79-0.96 (n=10); *Queen* HW 0.95-1.00 (n=3).

Biology. This species occurs in cloud forest habitats from 1430-2190 m elevation. Most specimens are from Winkler samples of sifted leaf litter and rotten wood. Workers and dealate queens occur in litter samples. A male is known from beating low vegetation. A few workers were collected at a cookie bait on the forest floor.

Etymology. The new species name is in reference to its being the largest member of the *C. gilva* complex. It is a noun in aposition and invariant.

Comments. *Cryptopone gilvagrande* can be separated from its sister clade, *C. gilva* + *C. guatemalensis*, by a relatively narrow petiolar node (Fig. 8A). It is sympatric with *C. guatemalensis*, and within its range, the two species have non-overlapping size distributions. However, some specimens of *C. guatemalensis* from north of the Isthmus of Tehuantepec are in the size range of *C. gilvagrande*.

Among the 6 COI barcodes for this species, the maximum intraspecific pairwise distance was 6%, and the smallest interspecific distance was 9%.

Cryptopone gilvatumida, New Species

(Figs. 6[map],8,9,11)

(Zoobank LSID: urn:lsid:zoobank.org:act:60FAE1DD-C54C-464F-B550-CFEB9CF039E1)

Type material. *Holotype worker*: Mexico, Veracruz, 12km WSW Xalapa, 19.52307 -97.02789 ± 20 m, 1940 m, 12 July 2016, cloud forest clearing, nest in dead wood (J. Longino #9738) [UNAM, unique specimen identifier CASENT0631951]. *Paratypes*: same data as holotype [1 worker, CAS, CASENT0644254; 1 worker, USNM, CASENT0644255]; same data except J. Longino #9739.2 [1 worker, MCZC, CASENT0644259; 1 worker, UCDC, CASENT0644260; 1 worker, IEXA, CASENT0644261; 1 worker, JTLC, CASENT0644262]; same data except J. Longino #9740 [3 workers, CAS, CASENT0644256, CASENT0644257, CASENT0644258].

Fig. 11. Holotype of *Cryptopone gilvatumida* (unique specimen identifier CASENT0631951).

Geographic range. Mexico (Puebla to Oaxaca).

Diagnosis. Petiolar node less tapering than *C. gilvagrande*, dorsally more rounded than *C. guatemalensis* (Fig. 8B and C); HW > 0.62.

Measurements. *Worker* HW 0.63-0.82 (n=10); *Queen* HW 0.87 (n=1).

Biology. This species occurs in cloud forest habitats from 1400-2040 m elevation. Most specimens are from Winkler samples of sifted leaf litter and rotten wood. Three nests were found in and under rotting wood in a small cloud forest clearing near Xalapa, Veracruz, Mexico. The larvae have five pairs of dorsal doorknob-shaped tubercles, as described for *C. gilva* (Wheeler and Wheeler 1952).

Etymology. The new species name is in reference to its being a member of the *C. gilva* complex and larger (more swollen) than sympatric populations of *C. guatemalensis*. It is a noun in aposition and invariant.

Comments. See comments under *C. guatemalensis* regarding the separation of *C. guatemalensis* and *C. gilvatumida*. Among the 3 COI barcodes for this species, the maximum intraspecific pairwise distance was 4%, and the smallest interspecific distance was 5%.

Fig. 12. Neotype of *Cryptopone guatemalensis* (unique specimen identifier CASENT0646802).

Cryptopone guatemalensis (Forel) Revived Status (Figs. 6[map],8,9,12)

Ponera ochracea r. *guatemalensis* Forel 1899:16. *Neotype worker* (**here designated**): Guatemala, Suchitepéquez: 4km S Vol. Atitlán, 14.54800 –91.19369 ± 200 m, 1570 m, cloud forest, ex rotten wood, 14 Jun 2009 (J. Longino #6709) [MHNG, unique specimen identifier CASENT0646802]. *Paraneotypes*: same data as holotype [1 worker, CAS, CASENT0646803; 1 alate queen, CAS, CASENT0646806; 1 male, CAS, CASENT0646809; 1 worker, MCZC, CASENT0646804; 1 alate queen, MCZC, CASENT0646807; 1 male, MCZC, CASENT0646810; 1 alate queen, USNM, CASENT0646805; 1 male, USNM, CASENT0646808].

Pachycondyla (*Pseudoponera*) *ochracea* r. *guatemalensis*: Emery, 1901:46.

Euponera (*Trachymesopus*) *ochracea* r. *guatemalensis*: Emery, 1911:86.

Trachymesopus ochracea r. *guatemalensis*: Kempf, 1960:424.

Cryptopone guatemalensis: Brown, 1963:6.

Euponera (*Trachymesopus*) *obsoleta* Menozzi 1931:196, fig. 5. Syntype worker: Costa Rica, Vara Blanca (Schmidt) [DEIC] (examined). Incorrect synonymy with *C. gilva* by Longino, 2006:135. New Synonymy.

Trachymesopus obsoleta: Kempf, 1960:424.

Pachycondyla obsoleta: Brown, in Bolton, 1995:308.

Pachycondyla gilva (part): Mackay & Mackay, 2010:352. Description of queen, male. Incorrect synonymy with *C. gilva*.

Geographic range. Mexico (Puebla) to Costa Rica.

Measurements. *Worker* HW 0.57-0.72 (n=26); *Queen* HW 0.72-0.83 (n=6).

Biology. This species occurs in cloud forest habitats from 940-1800 m elevation. Most specimens are from Winkler samples of sifted leaf litter and rotten wood. Workers and dealate queens occur in litter samples. Males are frequent in Malaise trap samples (B. Boudinot, personal communication). Nests are often encountered in and under loose bark of rotting wood on the forest floor, and under epiphyte mats near the ground in old treefalls. Colonies are diffusely spread in multiple chambers. Lone founding queens are commonly encountered. There is no evidence of polygyny (in contrast to *C. gilva)*.

Comments. It is challenging to separate *C. guatemalensis* from *C. gilvatumida*, sister taxa in the molecular phylogeny. The existence of two species was first suggested when two size classes of workers were observed in a single Winkler sample from the state of Puebla, Mexico. The size difference was small, and otherwise the workers were all very similar. Yet sequencing of a smaller specimen allied it with a widespread *C. guatemalensis* clade, while a larger specimen was in a separate clade with specimens from the mountains of Veracruz and Oaxaca. A series of Winkler samples were taken in roadside forest patches from Cuetzalan to Zacapoaxtla, a distance of 17 km, and ranging from 1270 to 1790 m. *Cryptopone* were found at four of the sites and could be separated into two forms: one with HW < 0.61 and the petiolar node slightly more truncate dorsally (Fig. 8D), and the other with HW > 0.63 and the petiolar node more evenly rounded (Fig. 8B). These forms were identified as *C. guatemalensis* and *C. gilvatumida*, respectively. Single specimens of *C. guatemalensis* were found at each of two small roadside patches at 1270 and 1400 m. A third site, also at 1400 m but a larger mature forest patch in a shaded ravine, contained both species together. The fourth site, a roadside patch at 1790 m, contained *C. gilvatumida*. The other two sequenced specimens that formed a clade with *C. gilvatumida* from Puebla were from montane sites near Xalapa, Veracruz, and the Sierra de Mazateca in Oaxaca. These latter specimens were also very large and had an evenly rounded petiolar node (e.g., Fig. 8C).

However, size alone does not always separate *C. guatemalensis* and *C. gilvatumida*. Ants tend to be larger and darker at higher elevations (Bishop et al. 2016), and both *C. guatemalensis* and *C. gilvatumida* appear to exhibit this pattern as intraspecific variation (Fig. 9). Among the Puebla collections of *C. gilvatumida*, specimens from the 1790 m site were larger and darker than the specimens from the 1400 m site (HW 0.65-0.75 vs. 0.57-0.61; Fig. 9 D, E). In montane sites near Xalapa, Veracruz, a site at 1480 m yielded a single worker with the rounded node of *C. gilvatumida* and HW 0.63. A nearby site at 2000 m, and the source of one of the sequenced specimens of *C. gilvatumida*, had HW 0.78-0.81 (Fig. 9F). Specimens from Sierra Mazateca, also the source of a sequenced specimen of *C. gilvatumida*, were from above 1700 m and had HW 0.69-0.82. The Sierra de Los Tuxtlas appears to have only *C. guatemalensis*. Specimens from 1100 to 1240 m cloud forest, one of which was sequenced, had HW 0.58-0.64 (Figs. 8E and 9B). A specimen from the peak of Volcán San Martín, at 1580 m, had HW 0.72 (Figs. 8F and 9C). This large specimen was sequenced and clustered closely with the specimen from downslope. South of the Isthmus of Tehuantepec, *C. guatemalensis* has HW 0.60-0.70, on average larger than specimens from Oaxaca northward.

Forel (1899) described *C. guatemalensis* based on material from Guatemala, Aceituna (Champion) and Nicaragua, Chontales (Janson). Mackay and Mackay (2010) designated a specimen at MHNG as lectotype. We examined this specimen and conclude it was not a syntype, and thus it cannot be a lectotype. The label indicates the specimen is from Florida in the United States, and the specimen has the measurements of true *C. gilva*. This is

presumably a specimen that was identified as *C. guatemalensis* by Forel after the publication of the name. This specimen has been given the specimen identifier CASENT0646799, and the images are on AntWeb. The lectotype label has been removed to avoid confusion.

No one has been able to locate the syntypes of *C. guatemalensis* and they are presumed lost. Longino searched MHNG in 1990, Mackay and Mackay at some later time, and Fisher's imaging crew recently. Likewise a search by curators at BMNH failed to locate the syntypes. Forel described the race as being smaller than *C. ochracea*. *Cryptopone ochracea* is smaller than typical *C. gilva*, and thus Forel's syntypes were probably the smaller of the two sympatric species in Guatemala, and not the larger one described here as *C. gilvagrande*. We thus establish a neotype for *C. guatemalensis*.

Among the 43 COI barcodes for this species, the maximum intraspecific pairwise distance was 8%, and the smallest interspecific distance was 5%.

Wadeura Weber 1939 Revived Status

Type species: *Wadeura guianensis* Weber, 1939:103; by original designation.

See discussion of morphology under *Cryptopone*. *Wadeura* now contains four species: *W. guianensis*, *W. holmgreni*, *W. holmgrenita* **sp. nov.**, and *W. pauli*. Phylogenetic information is available for three of the four known species, with *W. pauli* being sister to *W. holmgrenita* and *W. guianensis*. *Wadeura holmgreni* is very similar to *W. holmgrenita* and the two are likely sister species.

Key to workers of *Wadeura*

1 Mandible strongly falcate (Fig. 13A); ventral margin of petiole a deep, evenly convex lobe (Fig. 14A); common species from Mexico to Brazil and Peru ..... *guianensis*

- Mandible triangular (Fig. 13B–D); ventral margin of petiole less symmetrical (Fig. 14B–D); rare species from South America 2

2 Ventral margin of petiole a triangular lobe with pronounced anterior tooth (Fig. 14 B) ..... *pauli*

- Ventral margin of petiole a shallow lobe lacking anterior tooth (Fig. 14C and D)..... 3

3 Triangular projection of medial clypeus prominent, projecting beyond the outline of the clypeolabral juncture in full face view (Fig. 13C); HW > 0.8..... *holmgreni*

- Triangular projection of medial clypeus smaller, not projecting beyond the outline of the clypeolabral juncture (Fig. 13D); HW < 0.8..... *holmgrenita*

Wadeura guianensis Weber Revived Combination Figs. 13,14

Wadeura guianensis Weber 1939:103, figs. 5,6. Holotype worker: Guyana, Oronoque River of the Courantyne River basin, 2°42'N, 2 Aug. 1936 (N. Weber) [MCZC] (examined). *Pachycondyla guianensis*: Brown, in Bolton 1995:305; Mackay & Mackay, 2010:367 (description of queen, male). *Cryptopone guianensis*: Schmidt and Shattuck 2014:185.

Wadeura haskinsi Weber 1939:104, fig. 7. Holotype worker: Panama, Barro Colorado Island (C. P. Haskins) [MCZC] (examined). Kempf 1958:176-179, figs. 1–5 (description of queen). Synonymy under *Pachycondyla guianensis* by Mackay & Mackay, 2010:367.

Geographic range. Mexico (Veracruz) to Peru and Brazil.

Measurements. *Worker* HW 0.99-1.21 (n=5); *Queen* HW 1.18-1.27 (n=2).

Biology. Mackay and Mackay (2010) review the biology. The species occurs mainly in mature or secondary wet forests. It is a lowland species, with recorded elevational range sea level to 780 m, and the great majority of observations under 500 m. Workers are most often encountered in Winkler or Berlese samples of leaf litter and rotting wood. Males are relatively common in Malaise and light trap samples (B. Boudinot, personal communication), and alate queens occasionally occur in Malaise samples. Weber observed a nest as follows: "A small colony consisting of a half dozen workers, a queen and larvae was found a few centimeters down in sandy loam in high rain forest with many Brazil-nut trees (*Bertholletia excelsa* or *nobilis*). The nest was in the form of irregular chambers. The queen had a larger thorax than the workers and had evidently borne wings." Weber preserved a single worker from this nest, which became the holotype; the rest of the colony was lost. Kempf (1958) observed nests beneath bricks in sandy soil.

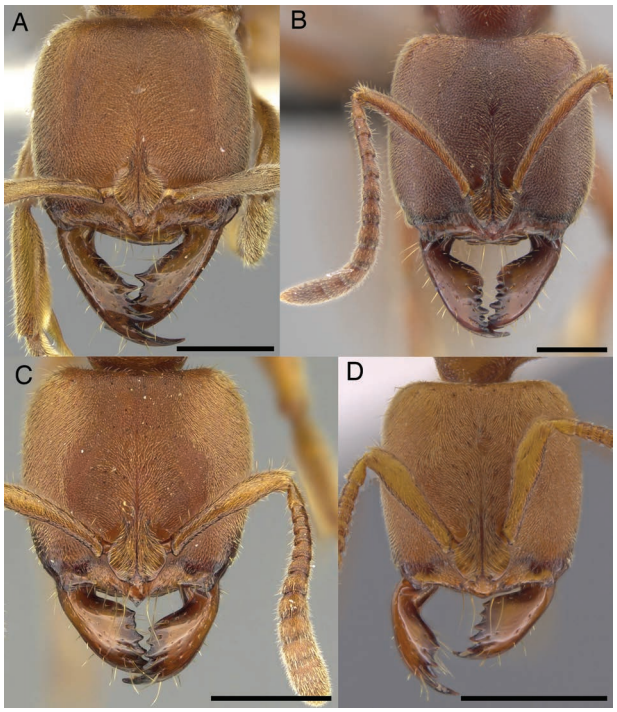

Fig. 13. *Wadeura* species, face views. (A) *W. guianensis* (image by R. Perry, CASENT0249146). (B) *W. pauli* (image by M. Pierce, CASENT0637806). (C) *W. holmgreni* (image by M. Esposito, CASENT0373370). (D) *W. holmgrenita* (CASENT0637779). Scale bars are 0.5 mm.

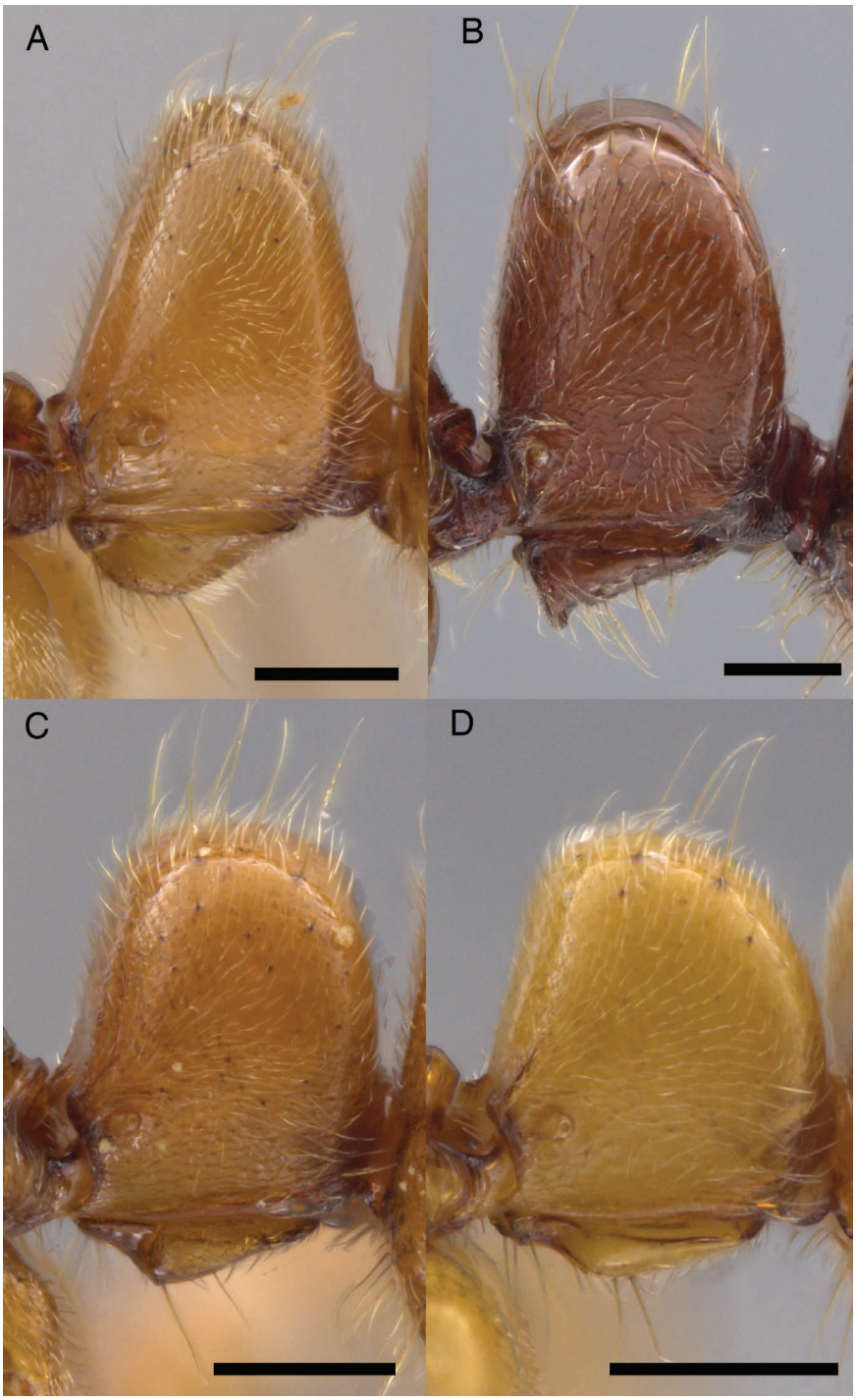

Fig. 14. *Wadeura* species, petiole lateral views. (A) *W. guianensis* (CASENT0640150). (B) *W. pauli* (CASENT0637806). (C) *W. holmgreni* (CASENT0373370). (D) *W. holmgrenita* (CASENT0637779). Scale bars are 0.2 mm.

Wadeura holmgreni Wheeler New Combination

Figs. 13,14

Euponera (Trachymesopus) holmgreni Wheeler 1925:6. Holotype worker: Peru (N. Holmgren) [MCZC] (examined).
Trachymesopus holmgreni: Kempf, 1960:424; Kempf, 1961:494, figs. 4,5,6 (redescription of worker).
Pachycondyla holmgreni: Brown, in Bolton 1995:306; Mackay & Mackay, 2010:390.
Cryptopone holmgreni: Schmidt and Shattuck 2014:185.

Geographic range. Peru, Trinidad, Suriname, French Guiana, Brazil.

Measurements. *Worker* HW 0.84-0.95 (n=10); *Ergatoid queen (?)* HW 0.96 (n=1); *Queen* HW 1.07 (n=1). Eight of the worker measurements were made by P. S. Ward, of specimens from Brazil (Bahia) and French Guiana at CPDC. Ward also measured a putative ergatoid queen, a large female with several ommatidia (in contrast to the completely eyeless workers and the queen with fully-developed compound eyes). One measurement is Mackay and Mackay's report of 0.89 as the HW of the *C. holmgreni* holotype. Measurements of

one worker and one queen were made by us, on specimens from Peru. The Peruvian worker measured by us was the largest, at 0.95.

Biology. The few records of this species are from lowland rainforest. Most records are from below 500 m elevation. Fisher and Esteves collected workers in soil at a rainforest site in Peru, at 650 m elevation.

Wadeura holmgrenita, New Species (Figs. 13,14,15)

(Zoobank LSID: urn:lsid:zoobank.org:act:7E5A70E9-2F48-4200-9EA0-4544436F5DA5)

Type material. *Holotype worker*: Peru, Madre de Dios: Estación Biológica Villa Carmen, 12.8753 -71.41095 ± 300 m, 650 m, 21 Oct 2015, rainforest, in soil (B.L.Fisher, F.A.Esteves # BLF31580) [MUSM, unique specimen identifier CASENT0637779]. Paratypes, same data as holotype [1 worker, CAS, CASENT0370848; 1 worker, MCZC, CASENT0370849; 1 worker, MZSP, CASENT0370850]; same data except collection number BLF31570 [1 worker, UCDC, CASENT0370863; 1 worker, JTLC, CASENT0370864]; same data except collection number BLF31572 [1 worker, USNM, CASENT0370865].

Geographic range. Peru (Madre de Dios).

Diagnosis. Mandible subtriangular, not extremely falcate (unlike *W. guianensis*); triangular projection of medial clypeus not projecting beyond the outline of the clypeolabral juncture (unlike *W. holmgreni*); ventral petiolar margin a shallow, subangular lobe (unlike *W. guianensis* and *W. pauli*); HW 0.66-0.73 (smaller than all other species).

Measurements. *Worker* HW 0.66-0.73 (n=9); *Ergatoid queen (?)* HW 0.75-0.78 (n=3).

Biology. All specimens of this species are from Estación Biológica Villa Carmen, from five collections by Fisher & Esteves. Habitats were rainforest, bamboo forest, second growth vegetation, and clearings. Four collections were in soil, one from under a stone.

Etymology. The new species name is in reference to its being a small version of *W. holmgreni*. It is a noun in aposition and invariant.

Comments. Alate queens are unknown in this species but that may be a consequence of undersampling. Three individuals from one collection are worker-like, but they are the largest of all measured individuals, and they have small compound eyes near the mandibular insertions. The eyes are composed of 5–8 ommatidia. Another individual from this same collection is smaller and eyeless. The specimens with eyes may be ergatoid queens. A similar pattern, of small eyeless workers and larger worker-like individuals with eyes, is seen in *W. holmgreni*.

Wadeura pauli Fernandes & Delabie (New Combination) (Figs. 13,14)

Cryptopone pauli Fernandes & Delabie, 2019:409. Holotype worker: Brazil, Rondônia, Floresta Nacional do Jamari (Flona Jamari), 63°01'24"W 9°09'40"S, Serra da Onça, 29.v.2018, in soil sample (D.C. Castro) [INPA] (not examined).
Sequenced specimen: Guyana, Potaro-Siparuni: 8km WNW Chenapau, 5.00851 –59.64133 ± 20 m, 510 m, 13 Oct 2015, premontane rainforest, ex sifted leaf litter (M. G. Branstetter #MGB2118).

Measurements. *Worker* HW 1.41 (holotype), 1.46 (sequenced specimen).

Comments. This species is by far the largest in the genus. It is now known from six specimens: the holotype and three paratypes from Rondônia, the sequenced specimen from Guyana, and a specimen from Rio Trombetas, Pará, Brazil (imaged specimen ANTWEB1041391 on AntWeb). The sequenced specimen has a tiny compound eye, raising the possibility that it is an ergatoid queen. *Wadeura holgreni* and *W. holmgrenita* have both completely eyeless workers and worker-like individuals with tiny compound eyes. The latter are potentially ergatoid queens.

Fisheropone hartwigi (Arnold) New Combination

Cryptopone hartwigi Arnold, 1948:213, figs. 2, 2a, 2b. Syntype worker: South Africa, Pretoria (E.K. Hartwig) [SAMC] (not examined). Combination in *Hypoponera*: Taylor, 1967:12. Combination in *Cryptopone*, status as species: Bolton, 1995: 166.

Comments. This species is transferred based on molecular evidence and no attempt is made to provide morphological evidence or to revise the diagnosis of the genus *Fisheropone*. The transfer serves mainly to exclude the species from *Cryptopone*.

Fig. 15. Holotype of *Wadeura holmgrenita* (CASENT0637779), lateral and dorsal views. Scale is the same for both images.

Centromyrmex brachycola (Roger)

Ponera brachycola Roger, 1861:5. Combination in *Centromyrmex*: Emery, 1890a:74; Emery, 1890b:40 (footnote); Kempf 1967:405.
Pachycondyla mirabilis Mackay & Mackay, 2010:466, figs. 5, 161, 586-588. Holotype worker: Bolivia, Rosario on Lake Rocagua (W. M. Mann) [LACM] (examined). Combination in *Cryptopone*: Schmidt and Shattuck 2014:185. **New Synonymy**.

Comments. Kempf (1967) reviewed the Neotropical *Centromyrmex*. Under *C. brachycola* he discussed a series from Bolivia, Rosario on Lake Rocagua, collected by Mann. Kempf referred to Mann's account of finding this colony in a termite mound (Mann 1934:189). Parts of this series are in multiple collections, including LACM. Mackay and Mackay observed specimens of this series at LACM and mistakenly described it as the new species *Pachycondyla mirabilis*, close to *W. gilva* and *W. holmgreni*.

Supplementary Data

Supplemental data are available at *Insect Systematics and Diversity* online.

Molecular Data Availability

Raw Illumina reads and contigs representing UCE loci have been deposited at the NCBI Sequence Read Archive and GenBank, respectively (BioProject# PRJNA778536). All newly generated COI sequences have been deposited at GenBank (OL439127-OL439155). A complete list of relevant NCBI accession numbers are available in Supp Table 4 (online only). All UCE and mtDNA matrices, all Trinity and SPAdes contigs, all tree files, unfiltered UCE alignments, and additional data analysis files (partitioning schemes, log files, etc.) have been deposited at Dryad (https://doi.org/10.5061/dryad.2280gb5t9). The Phyluce package and associated programs can be downloaded from github (github.com/faircloth-lab/phyluce). The ant-specific baits used to enrich UCE loci can be purchased from Arbor Biosciences (https://arborbiosci.com/genomics/targeted-sequencing/mybaits/mybaits-expert/mybaits-expert-uce/) and the UCE bait sequence file is available at figshare (https://figshare.com/articles/dataset/Hymenoptera_UCE_and_Exon_bait_sets_from_Branstetter_et_al_2017_/4630375).

Acknowledgments

We are very grateful to the ADMAC field team of 2015, who contributed to the lab work for this project: Irene Calderón, Josue Corrales, Krissy Dominguez, Scott Heacox, Josh Kouri, Irene Mata, Mac Pierce, and Marianela Solís. Rodolfo Probst and Ligia Benavides also contributed to the laboratory work. Hundreds of students and other collaborators contributed to field sampling from Mexico to Nicaragua. Additional specimens were provided by Bob Anderson, Doug Booher, Lech Borowiec, Brian Fisher, and Sebastian Salata. The manuscript benefited from comments of three reviewers. This project was supported by National Science Foundation grant DEB-1354739 (Project ADMAC) and most recently DEB-1932405 (Ants of the World), National Geographic Society Committee for Research and Exploration Grant 9568-14, and the University of Costa Rica (Vicerrectoría de Investigación, Project No.810-B4-531). USDA is an equal opportunity provider and employer.

Specimen Collection Statement

We support compliance with the Nagoya Protocol (https://www.cbd.int/abs/doc/protocol/nagoya-protocol-en.pdf). The authors attest that for all relevant specimens used in this study all legal and regulatory requirements, including export and import collection permits, have been followed for the collection of specimens from source populations at any international, national, regional or other geographic level.

References Cited

Alatorre-Bracamontes, C. E., and M. Vásquez-Bolaños. 2010. Lista comentada de las hormigas (Hymenoptera: Formicidae) del norte de México. Dugesiana 17: 9–36.

Allio, R., A. Schomaker-Bastos, J. Romiguier, F. Prosdocimi, B. Nabholz, and F. Delsuc. 2020. MitoFinder: efficient automated large-scale extraction of mitogenomic data in target enrichment phylogenomics. Mol. Ecol. Resour. 20: 892–905.

Andermann, T., A. M. Fernandes, U. Olsson, M. Töpel, B. Pfeil, B. Oxelman, A. Aleixo, B. C. Faircloth, and A. Antonelli. 2019. Allele phasing greatly improves the phylogenetic utility of ultraconserved elements. Syst. Biol. 68: 32–46.

Arbogast, B. S. 2007. A brief history of the New World flying squirrels: phylogeny, biogeography, and conservation genetics. J. Mammal. 88: 840–849.

Arnold, G. 1948. New species of African Hymenoptera. No. 8. Occas. Pap. Natl. Mus. South. Rhod. 2: 213–250.

Axelrod, D. I. 1975. Evolution and biogeography of Madrean-Tethyan sclerophyll vegetation. Ann. Mo. Bot. Gard. 62: 280–334.

Bankevich, A., S. Nurk, D. Antipov, A. A. Gurevich, M. Dvorkin, A. S. Kulikov, V. M. Lesin, S. I. Nikolenko, S. Pham, A. D. Prjibelski, et al. 2012. SPAdes: a new genome assembly algorithm and its applications to single-cell sequencing. J. Comput. Biol. 19: 455–477.

Bishop, T. R., M. P. Robertson, H. Gibb, B. J. van Rensburg, B. Braschler, S. L. Chown, S. H. Foord, T. C. Munyai, I. Okey, P. G. Tshivhandekano, et al. 2016. Ant assemblages have darker and larger members in cold environments. Glob. Ecol. Biogeogr. 25: 1489–1499.

Bolger, A. M., M. Lohse, and B. Usadel. 2014. Trimmomatic: a flexible trimmer for Illumina sequence data. Bioinformatics. 30: 2114–2120.

Bolton, B. 1995. A New General Catalogue of the Ants of the World. Harvard University Press, Cambridge, MA.

Bolton, B. 2021. An online catalog of the ants of the world. Available from http://antcat.org (accessed June 2, 2021).

Borowiec, M. L., C. Rabeling, S. G. Brady, B. L. Fisher, T. R. Schultz, and P. S. Ward. 2019. Compositional heterogeneity and outgroup choice influence the internal phylogeny of the ants. Mol. Phylogenet. Evol. 134: 111–121.

Bouckaert, R., J. Heled, D. Kühnert, T. Vaughan, C. H. Wu, D. Xie, M. A. Suchard, A. Rambaut, and A. J. Drummond. 2014. BEAST 2: a software platform for Bayesian evolutionary analysis. Plos Comput. Biol. 10: e1003537.

Brady, S. G., T. R. Schultz, B. L. Fisher, and P. S. Ward. 2006. Evaluating alternative hypotheses for the early evolution and diversification of ants. Proc. Natl. Acad. Sci. U. S. A. 103: 18172–18177.

Branstetter, M. G. 2012. Origin and diversification of the cryptic ant genus *Stenamma* Westwood (Hymenoptera: Formicidae), inferred from multilocus molecular data, biogeography and natural history. Syst. Entomol. 37: 478–496.

Branstetter, M. G. 2013. Revision of the Middle American clade of the ant genus *Stenamma* Westwood (Hymenoptera, Formicidae, Myrmicinae). ZooKeys 295: 1–277.

Branstetter, M. G., and J. Longino. 2019. UCE phylogenomics of New World *Ponera* Latreille (Hymenoptera: Formicidae) illuminates the origin and phylogeographic history of the endemic exotic ant *P. exotica*. Insect Syst. Divers. 3: 1–13.

Branstetter, M. G., J. T. Longino, P. S. Ward, and B. C. Faircloth. 2017. Enriching the ant tree of life: enhanced UCE bait set for genome-scale phylogenetics of ants and other Hymenoptera. Methods Ecol. Evol. 8: 768–776.

Braun, E. L. 1950. Deciduous Forests of Eastern North America. Blakiston, Philadelphia, PA.

Brown, W. L., Jr. 1963. Characters and synonymies among the genera of ants. Part III. Some members of the tribe Ponerini (Ponerinae, Formicidae). Breviora 190: 1–10.

Bryant, D., R. Bouckaert, J. Felsenstein, N. A. Rosenberg, and A. RoyChoudhury. 2012. Inferring species trees directly from biallelic genetic markers: bypassing gene trees in a full coalescent analysis. Mol. Biol. Evol. 29: 1917–1932.

Bush, M. B., and H. Hooghiemstra. 2005. Tropical biotic responses to climate change, pp. 125–137. In T. E. Lovejoy and L. Hannah (eds.), Climate Change and Biodiversity. Yale University Press, New Haven, CT.

Carlton, C. E. 1990. Biogeographic affinities of Pselaphid beetles of the Eastern United States. Fla. Entomol. 73: 570–579.

Creighton, W. S., and G. S. Tulloch. 1930. Notes on *Euponera gilva (*Roger) (Hymenoptera, Formicidae). Psyche 37: 71–79.

Deevey, E. S. 1949. Biogeography of the pleistocene. Bull. Geol. Soc. Am. 60: 1315–1416.

Dlussky, G. 2009. The ant subfamilies Ponerinae, Cerapachyinae, and Pseudomyrmecinae (Hymenoptera, Formicidae) in the late Eocene ambers of Europe. Paleontol. J. 43: 1043–1086.

Economo, E. P., N. Narula, N. R. Friedman, M. D. Weiser, and B. Guénard. 2018. Macroecology and macroevolution of the latitudinal diversity gradient in ants. Nat. Commun. 9: 1778.

Emery, C. 1890a. Voyage de M. E. Simon au Venezuela (Décembre 1887 - Avril 1888). Formicides. Ann. Soc. Entomol. France 10(6): 55–76.

Emery, C. 1890b. Studii sulle formiche della fauna neotropica. Bull. Soc. Entomol. Ital. 22: 38–80, Tav. V-IX.

Emery, C. 1893 (1892). [Untitled. Introduced by: "M. C. Emery, de Bologne, envoie les diagnoses de cinq nouveaux genres de Formicides".]. Bull. Bimens. Soc. Entomol. Fr. 1892: cclxxv–cclxxvii.

Emery, C. 1901. Notes sur les sous-familles des Dorylines et Ponérines (Famille des Formicides). Ann. Soc. Entomol. Belg. 45: 32–54.

Emery, C. 1911. Hymenoptera. Fam. Formicidae. Subfam. Ponerinae, vol. 118, Brussels.

Faircloth, B. 2013. Illumiprocessor: a trimmomatic wrapper for parallel adapter and quality trimming. Available at: https://doi.org/10.6079/J9ILL.

Faircloth, B. C. 2016. PHYLUCE is a software package for the analysis of conserved genomic loci. Bioinformatics. 32: 786–788.

Faircloth, B. C., J. E. McCormack, N. G. Crawford, M. G. Harvey, R. T. Brumfield, and T. C. Glenn. 2012. Ultraconserved elements anchor thousands of genetic markers spanning multiple evolutionary timescales. Syst. Biol. 61: 717–726.

Faircloth, B. C., M. G. Branstetter, N. D. White, and S. G. Brady. 2015. Target enrichment of ultraconserved elements from arthropods provides a genomic perspective on relationships among Hymenoptera. Mol. Ecol. Resour. 15: 489–501.

Fernandes, I. O., and J. H. Delabie. 2019. A new species of *Cryptopone* Emery (Hymenoptera: Formicidae: Ponerinae) from Brazil with observations on the genus and a key for new word species. Sociobiology 66: 408–413.

Flouri, T., X. Jiao, B. Rannala, and Z. Yang. 2018. Species tree inference with BPP using genomic sequences and the multispecies coalescent. Mol. Biol. Evol. 35: 2585–2593.

Forel, A. 1899. Formicidae. [part a], pp. 1–24, Insecta. Hymenoptera. Formicidae, vol. 3. R.H. Porter, Dulau & Co., London.

Grabherr, M. G., B. J. Haas, M. Yassour, J. Z. Levin, D. A. Thompson, I. Amit, X. Adiconis, L. Fan, R. Raychowdhury, Q. Zeng, et al. 2011. Full-length transcriptome assembly from RNA-Seq data without a reference genome. Nat. Biotechnol. 29: 644–652.

Graham, A. 1999. The Tertiary history of the northern temperate element in the northern Latin American biota. Am. J. Bot. 86: 32–38.

Guindon, S., J. F. Dufayard, V. Lefort, M. Anisimova, W. Hordijk, and O. Gascuel. 2010. New algorithms and methods to estimate maximum-likelihood phylogenies: assessing the performance of PhyML 3.0. Syst. Biol. 59: 307–321.

Halffter, G. 1987. Biogeography of the montane entomofauna of Mexico and Central-America. Annu. Rev. Entomol. 32: 95–114.

Harris, R. S. 2007. Improved pairwise alignment of genomic DNA. Ph.D. thesis, Pennsylvania State University, PA.

Haskins, C. P. 1931. Notes on the biology and social life of *Euponera gilva* Roger var. *harnedi* M. R. Smith. J. N. Y. Entomol. Soc. 39: 507–521.

Hoang, D. T., O. Chernomor, A. von Haeseler, B. Q. Minh, and L. S. Vinh. 2018. UFBoot2: improving the ultrafast bootstrap approximation. Mol. Biol. Evol. 35: 518–522.

Jackson, N. D., B. C. Carstens, A. E. Morales, and B. C. O'Meara. 2017. Species delimitation with gene flow. Syst. Biol. 66: 799–812.

Junier, T., and E. M. Zdobnov. 2010. The Newick utilities: high-throughput phylogenetic tree processing in the UNIX shell. Bioinformatics. 26: 1669–1670.

Kalyaanamoorthy, S., B. Q. Minh, T. K. F. Wong, A. von Haeseler, and L. S. Jermiin. 2017. ModelFinder: fast model selection for accurate phylogenetic estimates. Nat. Methods. 14: 587–589.

Katoh, K., and D. M. Standley. 2013. MAFFT multiple sequence alignment software version 7: improvements in performance and usability. Mol. Biol. Evol. 30: 772–780.

Kempf, W. W. 1958. Discovery of the ant genus *Wadeura* in Brazil (Hymenoptera: Formicidae). Rev. Bras. Entomol. 8: 175–180.

Kempf, W. W. 1960. Miscellaneous studies on Neotropical ants (Hymenoptera, Formicidae). Stud. Entomol. (n.s.) 3: 417–466.

Kempf, W. W. 1961. A survey of the ants of the soil fauna in Surinam (Hymenoptera: Formicidae). Stud. Entomol. 4: 481–524.

Kempf, W. W. 1967 (1966). A synopsis of the Neotropical ants of the genus *Centromyrmex* Mayr (Hymenoptera: Formicidae). Stud. Entomol. 9: 401–410.

Kim, J., and M. J. Sanderson. 2008. Penalized likelihood phylogenetic inference: bridging the parsimony-likelihood gap. Syst. Biol. 57: 665–674.

Lanfear, R., B. Calcott, S. Y. Ho, and S. Guindon. 2012. Partitionfinder: combined selection of partitioning schemes and substitution models for phylogenetic analyses. Mol. Biol. Evol. 29: 1695–1701.

Lanfear, R., P. B. Frandsen, A. M. Wright, T. Senfeld, and B. Calcott. 2017. PartitionFinder 2: new methods for selecting partitioned models of evolution for molecular and morphological phylogenetic analyses. Mol. Biol. Evol. 34: 772–773.

Larabee, F. J., B. L. Fisher, C. A. Schmidt, P. Matos-Maraví, M. Janda, and A. V. Suarez. 2016. Molecular phylogenetics and diversification of trap-jaw ants in the genera *Anochetus* and *Odontomachus* (Hymenoptera: Formicidae). Mol. Phylogenet. Evol. 103: 143–154.

Longino, J. T. 2006. New species and nomenclatural changes for the Costa Rican ant fauna (Hymenoptera: Formicidae). Myrmecol. Nachr. 8: 131–143.

Longino, J. T., and M. G. Branstetter. 2020. Phylogenomic species delimitation, taxonomy, and 'bird guide' identification for the Neotropical ant genus *Rasopone* (Hymenoptera: Formicidae). Insect Syst. Divers. 4: 1.

MacKay, W. P., and E. MacKay. 2010. The Systematics and Biology of the New World Ants of the Genus *Pachycondyla* (Hymenoptera: Formicidae). Edwin Mellen Press, Lewiston, New York.

Mann, W. M. 1934. Stalking ants, savage and civilized. Natl. Geogr. Mag. 66: 171–192.

Matos-Maraví, P., N. J. Matzke, F. J. Larabee, R. M. Clouse, W. C. Wheeler, D. M. Sorger, A. V. Suarez, and M. Janda. 2018. Taxon cycle predictions supported by model-based inference in Indo-Pacific trap-jaw ants (Hymenoptera: Formicidae: *Odontomachus*). Mol. Ecol. 27: 4090–4107.

Menozzi, C. 1931. Qualche nuova formica di Costa Rica (Hym.). Stett. Entomol. Ztg. 92: 188–202.

Miller, M. A., W. Pfeiffer, and T. Schwartz. 2010. Creating the CIPRES science gateway for inference of large phylogenetic trees, pp. 1–8, Proceedings of the Gateway Computing Environments Workshop (GCE). IEEE, New Orleans.

Minh, B. Q., M. A. Nguyen, and A. von Haeseler. 2013. Ultrafast approximation for phylogenetic bootstrap. Mol. Biol. Evol. 30: 1188–1195.

Moreau, C. S., C. D. Bell, R. Vila, S. B. Archibald, and N. E. Pierce. 2006. Phylogeny of the ants: diversification in the age of angiosperms. Science. 312: 101–104.

Morris, A. B., S. M. Ickert-Bond, D. B. Brunson, D. E. Soltis, and P. S. Soltis. 2008. Phylogeographical structure and temporal complexity in American sweetgum (*Liquidambar styraciflua*; Altingiaceae). Mol. Ecol. 17: 3889–3900.

Morris, A. B., C. H. Graham, D. E. Soltis, and P. S. Soltis. 2010. Reassessment of phylogeographical structure in an eastern North American tree using Monmonier's algorithm and ecological niche modeling. J. Biogeogr. 37: 1657–1667.

Nguyen, L. T., H. A. Schmidt, A. von Haeseler, and B. Q. Minh. 2015. IQ-TREE: a fast and effective stochastic algorithm for estimating maximum-likelihood phylogenies. Mol. Biol. Evol. 32: 268–274.

Ohnishi, H., H. T. Imai, and M. T. Yamamoto. 2003. Molecular phylogenetic analysis of ant subfamily relationship inferred from rDNA sequences. Genes Genet. Syst. 78: 419–425.

Ouellette, G. D., B. L. Fisher, and D. J. Girman. 2006. Molecular systematics of basal subfamilies of ants using 28S rRNA (Hymenoptera: Formicidae). Mol. Phylogenet. Evol. 40: 359–369.

Paradis, E. 2013. Molecular dating of phylogenies by likelihood methods: a comparison of models and a new information criterion. Mol. Phylogenet. Evol. 67: 436–444.

Paradis, E., J. Claude, and K. Strimmer. 2004. APE: analyses of phylogenetics and evolution in R language. Bioinformatics. 20: 289–290.

Perkovsky, E., A. Rasnitsyn, A. Vlaskin, and M. Taraschuk. 2007. A comparative analysis of the Baltic and Rovno amber arthropod faunas: representative samples. Afr. Invertebr. 48: 229–245.

Phillips, M. J., and D. Penny. 2003. The root of the mammalian tree inferred from whole mitochondrial genomes. Mol. Phylogenet. Evol. 28: 171–185.

Pierce, M. P., M. G. Branstetter, and J. T. Longino. 2017. Integrative taxonomy reveals multiple cryptic species within Central American *Hylomyrma* FOREL, 1912 (Hymenoptera: Formicidae). Myrmecol. News 25: 131–143.

Prebus, M. M. 2021. Phylogenomic species delimitation in the ants of the *Temnothorax salvini* group (Hymenoptera: Formicidae): an integrative approach. Syst. Ent. 46: 307–326.

R Core Development Team. **2019**. R: A language and environment for statistical computing computer program. Vienna, Austria.

Rabiee, M., and S. Mirarab. 2021. SODA: multi-locus species delimitation using quartet frequencies. Bioinformatics 36: 5623–5631.

Rambaut, A., A. J. Drummond, D. Xie, G. Baele, and M. A. Suchard. 2018. Posterior summarization in bayesian phylogenetics using tracer 1.7. Syst. Biol. 67: 901–904.

Ratnasingham, S., and P. D. Hebert. 2007. bold: The Barcode of Life Data System (http://www.barcodinglife.org). Mol. Ecol. Notes. 7: 355–364.

Ritchie, A. M., N. Lo, and S. Y. Ho. 2017. The impact of the tree prior on molecular dating of data sets containing a mixture of inter-and intraspecies sampling. Syst. Biol. 66: 413–425.

Roger, J. 1861. Die Ponera-artigen Ameisen (Schluss). Berl. Entomol. Z. 5: 1–54.

Roger, J. 1863. Die neu aufgeführten Gattungen und Arten meines Formiciden-Verzeichnisses nebst Ergänzung einiger früher gegebenen Beschreibungen. Berl. Entomol. Z. 7: 131–214.

Ruiz-Sanchez, E., and J. F. Ornelas. 2014. Phylogeography of *Liquidambar styraciflua* (Altingiaceae) in Mesoamerica: survivors of a Neogene widespread temperate forest (or cloud forest) in North America? Ecol. Evol. 4: 311–328.

Schmidt, C. 2013. Molecular phylogenetics of ponerine ants (Hymenoptera: Formicidae: Ponerinae). Zootaxa. 3647: 201–250.

Schmidt, C. A., and S. O. Shattuck. 2014. The higher classification of the ant subfamily Ponerinae (Hymenoptera: Formicidae), with a review of ponerine ecology and behavior. Zootaxa 3817: 1–242.

Smith, M. R. 1929. Descriptions of five new North American ants, with biological notes. Ann. Entomol. Soc. Am. 22: 543–551.

Smith, M. R. 1934. Ponerine ants of the genus *Euponera* in the United States. Ann. Entomol. Soc. Am. 27: 557–564.

Smith, M. R. 1944. Additional ants recorded from Florida, with descriptions of two new subspecies. Florida Entomol. 27: 14–17.

Solís-Lemus, C., L. L. Knowles, and C. Ané. 2015. Bayesian species delimitation combining multiple genes and traits in a unified framework. Evolution. 69: 492–507.

Spagna, J. C., A. I. Vakis, C. A. Schmidt, S. N. Patek, X. Zhang, N. D. Tsutsui, and A. V. Suarez. 2008. Phylogeny, scaling, and the generation of extreme forces in trap-jaw ants. J. Exp. Biol. 211: 2358–2368.

Ströher, P. R., E. Zarza, W. Tsai, J. McCormack, R. Feitosa, and M. Pie. 2017. The mitochondrial genome of *Octostruma stenognatha* and its phylogenetic implications. Insectes Soc. 64: 149–154.

Sukumaran, J., and L. L. Knowles. 2017. Multispecies coalescent delimits structure, not species. Proc. Natl. Acad. Sci. U. S. A. 114: 1607–1612.

Tagliacollo, V. A., and R. Lanfear. 2018. Estimating improved partitioning schemes for ultraconserved elements. Mol. Biol. Evol. 35: 1798–1811.

Talavera, G., and J. Castresana. 2007. Improvement of phylogenies after removing divergent and ambiguously aligned blocks from protein sequence alignments. Syst. Biol. 56: 564–577.

Taylor, R. W. 1967. A monographic revision of the ant genus *Ponera* Latreille (Hymenoptera: Formicidae). Pac. Insects Monogr. 13: 1–112.

Vásquez-Bolaños, M. 2011. Lista de especies de hormigas (Hymenoptera: Formicidae) para México. Dugesiana 18: 95–133.

Ward, P. S., and M. G. Branstetter. 2017. The acacia ants revisited: convergent evolution and biogeographic context in an iconic ant/plant mutualism. Proc. R. Soc. Lond. B Biol. Sci. 284: 20162569.

Ward, P. S., and D. A. Downie. 2005. The ant subfamily Pseudomyrmecinae (Hymenoptera: Formicidae): phylogeny and evolution of big-eyed arboreal ants. Syst. Entomol. 30: 310–335.

Ward, P. S., and B. L. Fisher. 2016. Tales of dracula ants: the evolutionary history of the ant subfamily Amblyoponinae (Hymenoptera: Formicidae). Syst. Entomol. 41: 683–693.

Ward, P. S., S. G. Brady, B. L. Fisher, and T. R. Schultz. 2015. The evolution of myrmicine ants: phylogeny and biogeography of a hyperdiverse ant clade (Hymenoptera: Formicidae). Syst. Entomol. 40: 61–81.

Weber, N. A. 1939. New ants of rare genera and a new genus of ponerine ants. Ann. Entomol. Soc. Am. 32: 91–104.

Wheeler, W. M. 1925. Neotropical ants in the collections of the Royal Museum of Stockholm. Ark. Zool. 17A (8): 1–55.

Wheeler, W. M., and F. M. Gaige. 1920. *Euponera gilva* (Roger), a rare North American ant. Psyche 27: 69–72.

Wheeler, G. C., and J. Wheeler. 1952. The ant larvae of the subfamily Ponerinae - Part II. Am. Midl. Nat. 48: 604–672.

Wheeler, G. C., and J. Wheeler. 1985. A checklist of Texas ants. Prairie Nat. 17: 49–64.

Yang, Z. 2015. The BPP program for species tree estimation and species delimitation. Curr. Zool. 61: 854–865.

Zachos, J., M. Pagani, L. Sloan, E. Thomas, and K. Billups. 2001. Trends, rhythms, and aberrations in global climate 65 Ma to present. Science. 292: 686–693.

Zhang, J., P. Kapli, P. Pavlidis, and A. Stamatakis. 2013. A general species delimitation method with applications to phylogenetic placements. Bioinformatics. 29: 2869–2876.

Zhang, C., E. Sayyari, and S. Mirarab. 2017. ASTRAL-III: increased scalability and impacts of contracting low support branches, pp. 53–75, RECOMB International Workshop on Comparative Genomics, Springer.

Zhao, Y., Z. Qi, W. Ma, Q. Dai, P. Li, K. M. Cameron, J. Lee, Q.-Y. Xiang, and F. Chengxin. 2013. Comparative phylogeography of the *Smilax hispida* group (Smilaceae) in eastern Asia and North America – Implications for allopatric speciation, causes of diversity disparity, and origins of temperate elements in Mexico. Mol. Phylogenet. Evol. 68: 300–311.